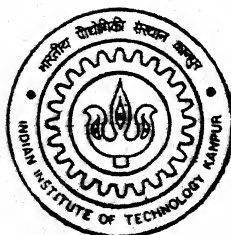


Simulation of Mixed Convection Cooling of PCBs—an Experimental Study

by

MANISH KUMAR



TH
ME/2001/M
K962

DEPARTMENT OF MECHANICAL ENGINEERING
INDIAN INSTITUTE OF TECHNOLOGY, KANPUR

February, 2001

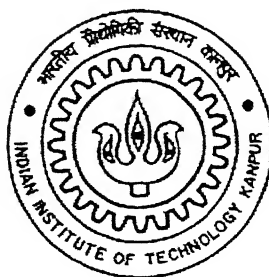
Simulation of Mixed Convection Cooling of PCBs – an Experimental Study

*A Thesis Submitted
In Partial Fulfillment of the Requirements
For the Degree of*

Master of Technology

by

Manish Kumar

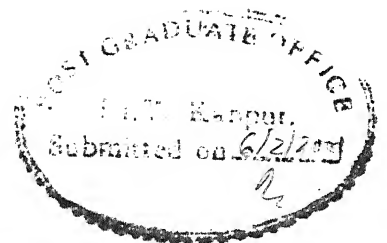


to the

**DEPARTMENT OF MECHANICAL ENGINEERING
INDIAN INSTITUTE OF TECHNOLOGY KANPUR**

FEBRUARY 2001

Certificate



It is certified that the work contained in the thesis entitled” **Simulation of Mixed Convection Cooling of PCBs-an Experimental Study** ” by **Mr. Manish Kumar**, has been carried out under my supervision and this work has not been submitted elsewhere for a degree.

Keshav Kant
05.02.2001
(Dr. Keshav Kant)

Professor,
Department of Mechanical Engineering,
Indian Institute of Technology,
Kanpur,
February, 2001

16 APR 2001/ME

केन्द्रीय पुस्तकालय
सा. प्र. वि. का. नमुर

अन्वेषण संख्या: A133714

TH
ME/2001/11

1991



A133714

Abstract

The objective of the present work was to develop an experimental test rig and to determine the heat transfer characteristics of a stack of vertical heated plates. The geometrical configuration designed and fabricated simulates the printed circuit boards (PCBs) used in various electronic devices. Attempts were made to find the optimum spacing between vertical plates (at which heat transfer will be maximum or increase in heat transfer afterwards will not be significant) and also the temperature distribution over the plates as the plate spacing and pressure difference across the channel were varied.

Uniform heat flux (UHF) model was adopted as both plates had the uniform heat generation. Heat flux from the plates is kept every time at a value such that temperature at any point should not exceed the prefixed temperature limit. Free as well as mixed convection cooling was observed for various pressure differences created by employing some suitable pressure difference-creating device at the top of the test section. The observations showed that for the particular pressure difference across the channel, the plate spacing had a significant effect on the heat transfer through PCBs. Furthermore, a noticeable trend was observed regarding power consumption to maintain the flow and total heat transferred from the plate surfaces. Data gathered through experiments was valuable in the sense that the currently adopted computational techniques for obtaining such data have to severely compromise with the actually occurring heat transfer and flow situations by making a lot of inescapable assumptions.

Contents

Certificate	: i
Acknowledgement	: ii
Abstract	: iii
Contents	: iv
Nomenclature	: v
List of Figures	: vi
Chapter -1 (General background)	: 1
Chapter -2 (Literature survey)	: 11
Chapter -3 (Problem formulation and experimental set-up requirements)	: 31
Chapter -4 (Modeling and apparatus design)	: 35
Chapter -5 (Results and discussion)	: 55
References	
Appendix 1	
Appendix 2	

Nomenclature

x	Plate spacing, mm
g	Gravitational acceleration, ms^{-2}
H	Plate height, mm
ΔP	Static pressure difference between top and bottom of the channel, Pa
Q_f	Heat flux, Wcm^{-2}
Q_t	Total heat transfer rate, kw
T_a	Ambient temperature, $^{\circ}\text{C}$
T^*	Non-dimensional temperature
T_e	Temperature at exit of the channel, $^{\circ}\text{C}$
W_f	Fan power, W
y	Distance along the plate measured from its bottom, mm
b^*	Non-dimensional thermocouple location at exit
b	Distance of thermocouple from one end at the channel exit, mm
B	Channel width at exit, mm
X	Maximum plate spacing, mm
Gr_y	Grashoff number measured along the plate
T_{top}	Temperature at the top of the plate, $^{\circ}\text{C}$
X_{opt}	Optimum plate spacing, mm
Q_{fopt}	Optimum heat flux, Wcm^{-2}
Re	Reynolds number
Sh	Sherwood number

List of Figures

- Figure 1.1** Typical configuration for natural convection cooling of electronics
- Figure 1.2** Factors affecting natural convection cooled PCBs
- Figure 1.3** Flow chart to be followed by a thermal designer
- Figure 2.1** Schematic diagram of the experimental set-up
- Figure 4.1a** Structural levels of an electronic computer
- Figure 4.1b** Primary components of a package
- Figure 4.2a** Experimental planning and execution process diagram
- Figure 4.2b** Block diagram representation of experimental test rig
- Figure 4.3** Schematic diagram of the experimental test rig
- Figure 4.4** Inlet section
- Figure 4.5** Test section
- Figure 4.6a** Thermocouple arrangement on front surface of heated plate (plate 1)
- Figure 4.6b** Cross-sectional view of heated plate
- Figure 4.6c** Thermocouple arrangement on front surface of heated plate (plate 2)
- Figure 4.7** Lead screw arrangement
- Figure 4.8** Diffuser
- Figure 4.9** Suction chamber
- Figure 4.10** Four types of honeycombs
- Figure 4.11** Thermocouple arrangement at test section inlet
- Figure 4.12** Thermocouple arrangement at test section exit
- Figure 5.1** Variation of plate heat flux with plate spacing for different static pressures

- Figure 5.2** Variation of total heat transfer with plate spacing for different static pressures
- Figure 5.3** Fan power variation with heat flux for different static pressures
- Figure 5.4** Variation of fan power with plate spacing for different static pressures
- Figure 5.5** Variation of air exit temperature with thermocouple location for different static pressures and plate spacing
- Figure 5.6** Variation of heat flux with optimum plate spacing
- Figure 5.7** Variation of optimum plate spacing with static pressure
- Figure 5.8** Variation of optimum heat flux with static pressure
- Figure 5.9** Three-dimensional variation of Gr with space co-ordinates for different static pressures
- Figure 5.10** Three dimensional variation of Gr with space co-ordinates for $\Delta P = 0.0$ Pa
- Figure 5.11** Three dimensional variation of Gr with space co-ordinates for $\Delta P = 4.4$ Pa
- Figure 5.12** Three dimensional variation of Gr with space co-ordinates for $\Delta P = 8.8$ Pa
- Figure 5.13** Three dimensional variation of Nu with space co-ordinates and static pressures
- Figure 5.14** Three dimensional variation of Nu with space co-ordinates for $\Delta P = 0.0$ Pa
- Figure 5.15** Three dimensional variation of Nu with space co-ordinates for $\Delta P = 4.4$ Pa
- Figure 5.16** Three dimensional variation of Nu with space co-ordinates for $\Delta P = 8.8$ Pa
- Figure 5.17** Three dimensional variation of Nu with space co-ordinates and static pressure

Chapter 1

GENERAL BACKGROUND

1.1 Introduction

Electronic equipment relies on flow and control of electrical current to perform a fantastic variety of functions. Whenever electrical current flows through a resistive element, heat is generated in that element. An increase in the current or in the resistance produces an increase in the amount of heat generated in the element. If the flow path is poor, the temperature may continue to rise until the resistive element destroys and the current stops flowing. If the heat flow path is good, the temperature may rise until it stabilizes at a point where the heat flowing away from the element is equal to the heat generated due to the electrical current flowing in the element.

Electronic systems, such as computers, televisions, digital multi-meters and signal conditioners are used for a variety of applications, most of which are not directly connected with fluid flow and heat transfer. But the cooling of electronic systems in order to ensure that temperature of the various components, particularly of the chips or semiconductor devices does not exceed the allowable temperature level is often the most crucial factor in the design and operation of the system. This is an important area for design since electronic devices are generally very temperature sensitive and it is crucial

to design efficient systems to dissipate the thermal energy generated in electronic equipments.

Apart from electrical current, rapid miniaturization of the size of electronic components has resulted in high surface heat fluxes, which have risen substantially from about 10^2 to 10^6 W/m². In short, the power has been increasing while the volume has been decreasing. This has produced a dramatic increase in the power density resulting in rapidly rising temperature. Further reduction in size is largely restricted by the heat transfer problems and availability of thermal systems to effectively cool the equipment.

1.2 Failure Modes

Important types of problems related with heat generation in electronic components are tabulated in table 1.1. The design process is generally first directed at the cooling parameters, keeping the geometry of the electronic circuitry unchanged. Therefore different fluids, flow rates, inlet fluid temperature and flow configurations are considered to determine if an acceptable design is obtained. If not the dimensions, number and locations may be varied; within the given constraints. If even this does not lead to an acceptable design the mode of cooling may be varied; for instance, going from natural to forced convection in air, to liquid immersion or to boiling.

1.3 Electronic Cooling by Natural Convection

Though natural convection has very low heat transfer coefficient, it is preferred for low -end applications because of its reliability and simplicity. In air, device heat fluxes are limited to roughly 0.1 W/cm² for allowable maximum temperature of 100^oC or the

Failure Mode	Characteristics
Soft Failures	<p>Circuit continues to operate, but does not meet specification when the temperature is elevated beyond the maximum operating temperature.</p> <p>Circuit returns to normal operation when temperature is lowered.</p> <p>Failure due to change in component parameters with temperature.</p>
Hard Failure (Short term)	<p>Circuit does not operate.</p> <p>Circuit may or may not return to normal operation when temperature is lowered. Failure is likely due to component or interconnection breakdown, but may also be due to change in component parameters with temperature.</p>
Hard Failure (Long term)	<p>Circuit does not operate at any temperature. Failures are irreversible.</p> <p>Failure may be caused by corrosion, inter metallic formation, or similar phenomenon. Failures may also be caused by mechanical stresses due to difference in temperature coefficient of expansion (TCE) between a component and the substrate.</p>

Table 1.1 Modes of Failure

order of $1\text{W}/\text{cm}^2$ maximum heat dissipation for a conventional encased chip module. Communication switching devices, avionics packages, electronic test equipment, consumer electronics and low-end computer packages are often cooled by natural convection in air. Figure 1.1 shows the typical configuration for natural convection cooling and figure 1.2 shows the factors affecting natural convection cooling.

1.4 Electronic Cooling by Forced Convection

Using fan, blower or a pump to provide high velocity fluid (air or liquid) past a heated surface so that we get less thermal resistance across the boundary layer of the fluid on the heated surface. This results in higher heat transfer rates and is called forced convection. Forced air systems can provide heat transfer rates in electronic systems that are 10 times greater than those available with natural convection and radiation. Forced liquid cooling systems can provide heat transfer rates that are 10 times greater than those for forced air cooling systems. This leads to increasing costs, power, noise and complexity. For liquid cooled systems the size and weight may also increase. Due to forced convection the size of air cooled system reduces with higher component densities and lower temperature of hot spots. This increases the electronic component reliability but requires added maintenance of the additional fans or pumps. A liquid cooled system is usually larger and heavier than an air-cooled system, because a reservoir is generally required for the liquid. A fan-cooled system, on the other hand, normally has a large supply of air readily available with no storage requirements, which reduces the size and weight of the system. Laminar flow conditions as well as turbulent flow conditions can exist with forced convection in liquid and air. Turbulent flow conditions are much more desirable, because

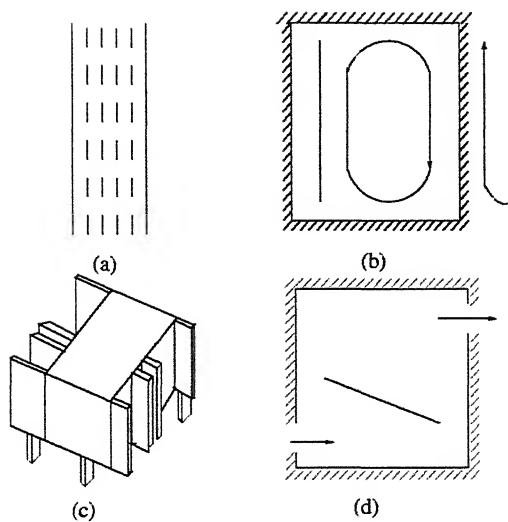


Figure 1.1 Typical Configuration For Natural Convection Cooling of Electronics
(a) Vertical Cabinet With Array of PCB's
(b) Sealed Enclosure,
(c) Externally Finned Enclosure
(d) Vented Enclosure With Horizontal PCB

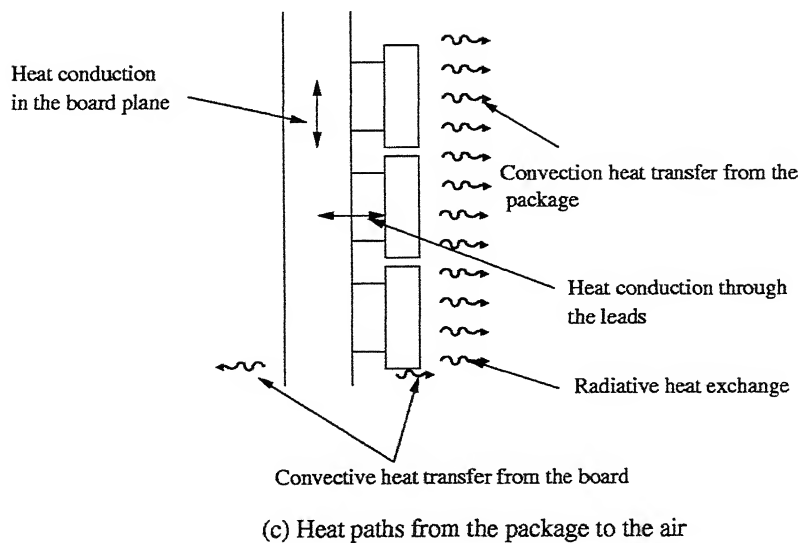
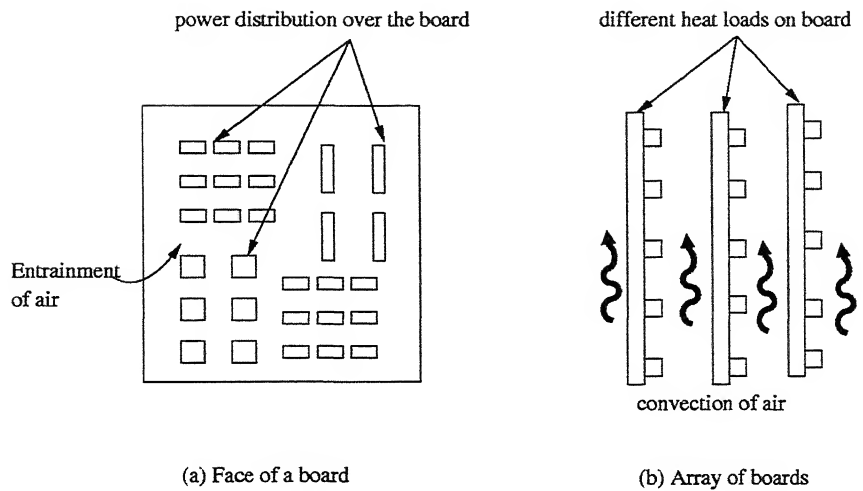


Figure 1.2 Factors Affecting Natural Convection Cooled PCB's.

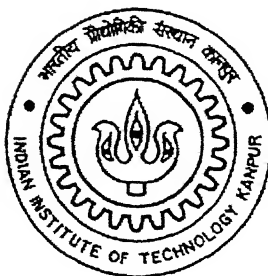
Simulation of Mixed Convection Cooling of PCBs – an Experimental Study

*A Thesis Submitted
In Partial Fulfillment of the Requirements
For the Degree of*

Master of Technology

by

Manish Kumar



to the

**DEPARTMENT OF MECHANICAL ENGINEERING
INDIAN INSTITUTE OF TECHNOLOGY KANPUR**

FEBRUARY 2001

7 APR 2001/ME

केन्द्रीय पुस्तकालय
सा. वि. वि. काजपुर

अवधि-1000 A133714

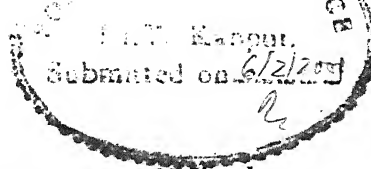
TH
ME/2001/11

1972

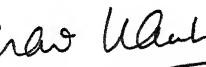


A133714

Certificate



certified that the work contained in the thesis entitled " **Simulation of Mixed
Convection Cooling of PCBs-an Experimental Study** " by **Mr. Manish Kumar**,
has been carried out under my supervision and this work has not been submitted
elsewhere for a degree.



05.02.2001
(Manish Kant)

Professor,
Department of Mechanical Engineering,
Indian Institute of Technology,
Kanpur,
February, 2001

Abstract

The objective of the present work was to develop an experimental test rig and to determine the heat transfer characteristics of a stack of vertical heated plates. The geometrical configuration designed and fabricated simulates the printed circuit boards (PCBs) used in various electronic devices. Attempts were made to find the optimum spacing between vertical plates (at which heat transfer will be maximum or increase in heat transfer afterwards will not be significant) and also the temperature distribution over the plates as the plate spacing and pressure difference across the channel were varied.

Uniform heat flux (UHF) model was adopted as both plates had the uniform heat generation. Heat flux from the plates is kept every time at a value such that temperature at any point should not exceed the prefixed temperature limit. Free as well as mixed convection cooling was observed for various pressure differences created by employing some suitable pressure difference-creating device at the top of the test section. The observations showed that for the particular pressure difference across the channel, the plate spacing had a significant effect on the heat transfer through PCBs. Furthermore, a noticeable trend was observed regarding power consumption to maintain the flow and total heat transferred from the plate surfaces. Data gathered through experiments was valuable in the sense that the currently adopted computational techniques for obtaining such data have to severely compromise with the actually occurring heat transfer and flow situations by making a lot of inescapable assumptions.

Contents

Certificate	: i
Acknowledgement	: ii
Abstract	: iii
Contents	: iv
Nomenclature	: v
List of Figures	: vi
Chapter -1 (General background)	: 1
Chapter -2 (Literature survey)	: 11
Chapter -3 (Problem formulation and experimental set-up requirements)	: 31
Chapter -4 (Modeling and apparatus design)	: 35
Chapter -5 (Results and discussion)	: 55
References	
Appendix 1	
Appendix 2	

Nomenclature

x	Plate spacing, mm
g	Gravitational acceleration, ms^{-2}
H	Plate height, mm
ΔP	Static pressure difference between top and bottom of the channel, Pa
Q_f	Heat flux, Wcm^{-2}
Q_t	Total heat transfer rate, kw
T_a	Ambient temperature, $^{\circ}\text{C}$
T^*	Non-dimensional temperature
T_e	Temperature at exit of the channel, $^{\circ}\text{C}$
W_f	Fan power, W
y	Distance along the plate measured from its bottom, mm
b^*	Non-dimensional thermocouple location at exit
b	Distance of thermocouple from one end at the channel exit, mm
B	Channel width at exit, mm
X	Maximum plate spacing, mm
Gr_y	Grashoff number measured along the plate
T_{top}	Temperature at the top of the plate, $^{\circ}\text{C}$
X_{opt}	Optimum plate spacing, mm
Q_{fopt}	Optimum heat flux, Wcm^{-2}
Re	Reynolds number
Sh	Sherwood number

List of Figures

- Figure 1.1** Typical configuration for natural convection cooling of electronics
- Figure 1.2** Factors affecting natural convection cooled PCBs
- Figure 1.3** Flow chart to be followed by a thermal designer
- Figure 2.1** Schematic diagram of the experimental set-up
- Figure 4.1a** Structural levels of an electronic computer
- Figure 4.1b** Primary components of a package
- Figure 4.2a** Experimental planning and execution process diagram
- Figure 4.2b** Block diagram representation of experimental test rig
- Figure 4.3** Schematic diagram of the experimental test rig
- Figure 4.4** Inlet section
- Figure 4.5** Test section
- Figure 4.6a** Thermocouple arrangement on front surface of heated plate (plate 1)
- Figure 4.6b** Cross-sectional view of heated plate
- Figure 4.6c** Thermocouple arrangement on front surface of heated plate (plate 2)
- Figure 4.7** Lead screw arrangement
- Figure 4.8** Diffuser
- Figure 4.9** Suction chamber
- Figure 4.10** Four types of honeycombs
- Figure 4.11** Thermocouple arrangement at test section inlet
- Figure 4.12** Thermocouple arrangement at test section exit
- Figure 5.1** Variation of plate heat flux with plate spacing for different static pressures

- Figure 5.2** Variation of total heat transfer with plate spacing for different static pressures
- Figure 5.3** Fan power variation with heat flux for different static pressures
- Figure 5.4** Variation of fan power with plate spacing for different static pressures
- Figure 5.5** Variation of air exit temperature with thermocouple location for different static pressures and plate spacing
- Figure 5.6** Variation of heat flux with optimum plate spacing
- Figure 5.7** Variation of optimum plate spacing with static pressure
- Figure 5.8** Variation of optimum heat flux with static pressure
- Figure 5.9** Three-dimensional variation of Gr with space co-ordinates for different static pressures
- Figure 5.10** Three dimensional variation of Gr with space co-ordinates for $\Delta P = 0.0$ Pa
- Figure 5.11** Three dimensional variation of Gr with space co-ordinates for $\Delta P = 4.4$ Pa
- Figure 5.12** Three dimensional variation of Gr with space co-ordinates for $\Delta P = 8.8$ Pa
- Figure 5.13** Three dimensional variation of Nu with space co-ordinates and static pressures
- Figure 5.14** Three dimensional variation of Nu with space co-ordinates for $\Delta P = 0.0$ Pa
- Figure 5.15** Three dimensional variation of Nu with space co-ordinates for $\Delta P = 4.4$ Pa
- Figure 5.16** Three dimensional variation of Nu with space co-ordinates for $\Delta P = 8.8$ Pa
- Figure 5.17** Three dimensional variation of Nu with space co-ordinates and static pressure

Chapter 1

GENERAL BACKGROUND

1.1 Introduction

Electronic equipment relies on flow and control of electrical current to perform a fantastic variety of functions. Whenever electrical current flows through a resistive element, heat is generated in that element. An increase in the current or in the resistance produces an increase in the amount of heat generated in the element. If the flow path is poor, the temperature may continue to rise until the resistive element destroys and the current stops flowing. If the heat flow path is good, the temperature may rise until it stabilizes at a point where the heat flowing away from the element is equal to the heat generated due to the electrical current flowing in the element.

Electronic systems, such as computers, televisions, digital multi-meters and signal conditioners are used for a variety of applications, most of which are not directly connected with fluid flow and heat transfer. But the cooling of electronic systems in order to ensure that temperature of the various components, particularly of the chips or semiconductor devices does not exceed the allowable temperature level is often the most crucial factor in the design and operation of the system. This is an important area for design since electronic devices are generally very temperature sensitive and it is crucial

to design efficient systems to dissipate the thermal energy generated in electronic equipments.

Apart from electrical current, rapid miniaturization of the size of electronic components has resulted in high surface heat fluxes, which have risen substantially from about 10^2 to 10^6 W/m². In short, the power has been increasing while the volume has been decreasing. This has produced a dramatic increase in the power density resulting in rapidly rising temperature. Further reduction in size is largely restricted by the heat transfer problems and availability of thermal systems to effectively cool the equipment.

1.2 Failure Modes

Important types of problems related with heat generation in electronic components are tabulated in table 1.1. The design process is generally first directed at the cooling parameters, keeping the geometry of the electronic circuitry unchanged. Therefore different fluids, flow rates, inlet fluid temperature and flow configurations are considered to determine if an acceptable design is obtained. If not the dimensions, number and locations may be varied; within the given constraints. If even this does not lead to an acceptable design the mode of cooling may be varied; for instance, going from natural to forced convection in air, to liquid immersion or to boiling.

1.3 Electronic Cooling by Natural Convection

Though natural convection has very low heat transfer coefficient, it is preferred for low -end applications because of its reliability and simplicity. In air, device heat fluxes are limited to roughly 0.1 W/cm² for allowable maximum temperature of 100^o C or the

Failure Mode	Characteristics
Soft Failures	<p>Circuit continues to operate, but does not meet specification when the temperature is elevated beyond the maximum operating temperature.</p> <p>Circuit returns to normal operation when temperature is lowered.</p> <p>Failure due to change in component parameters with temperature.</p>
Hard Failure (Short term)	<p>Circuit does not operate.</p> <p>Circuit may or may not return to normal operation when temperature is lowered. Failure is likely due to component or interconnection breakdown, but may also be due to change in component parameters with temperature.</p>
Hard Failure (Long term)	<p>Circuit does not operate at any temperature. Failures are irreversible.</p> <p>Failure may be caused by corrosion, inter metallic formation, or similar phenomenon. Failures may also be caused by mechanical stresses due to difference in temperature coefficient of expansion (TCE) between a component and the substrate.</p>

Table 1.1 Modes of Failure

order of $1\text{W}/\text{cm}^2$ maximum heat dissipation for a conventional encased chip module. Communication switching devices, avionics packages, electronic test equipment, consumer electronics and low-end computer packages are often cooled by natural convection in air. Figure 1.1 shows the typical configuration for natural convection cooling and figure 1.2 shows the factors affecting natural convection cooling.

1.4 Electronic Cooling by Forced Convection

Using fan, blower or a pump to provide high velocity fluid (air or liquid) past a heated surface so that we get less thermal resistance across the boundary layer of the fluid on the heated surface. This results in higher heat transfer rates and is called forced convection. Forced air systems can provide heat transfer rates in electronic systems that are 10 times greater than those available with natural convection and radiation. Forced liquid cooling systems can provide heat transfer rates that are 10 times greater than those for forced air cooling systems. This leads to increasing costs, power, noise and complexity. For liquid cooled systems the size and weight may also increase. Due to forced convection the size of air cooled system reduces with higher component densities and lower temperature of hot spots. This increases the electronic component reliability but requires added maintenance of the additional fans or pumps. A liquid cooled system is usually larger and heavier than an air-cooled system, because a reservoir is generally required for the liquid. A fan-cooled system, on the other hand, normally has a large supply of air readily available with no storage requirements, which reduces the size and weight of the system. Laminar flow conditions as well as turbulent flow conditions can exist with forced convection in liquid and air. Turbulent flow conditions are much more desirable, because

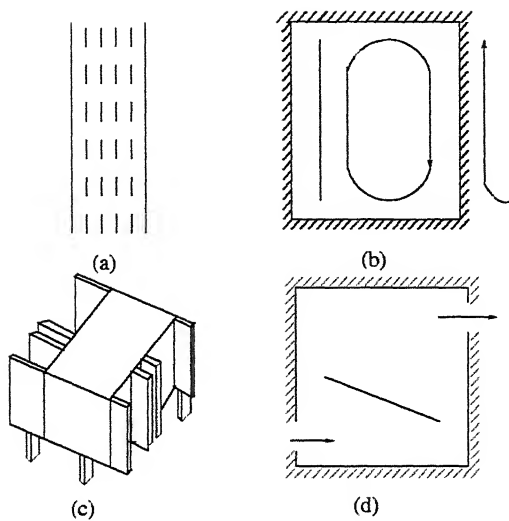


Figure 1.1 Typical Configuration For Natural Convection Cooling of Electronics
(a) Vertical Cabinet With Array of PCB's
(b) Sealed Enclosure,
(c) Externally Finned Enclosure
(d) Vented Enclosure With Horizontal PCB

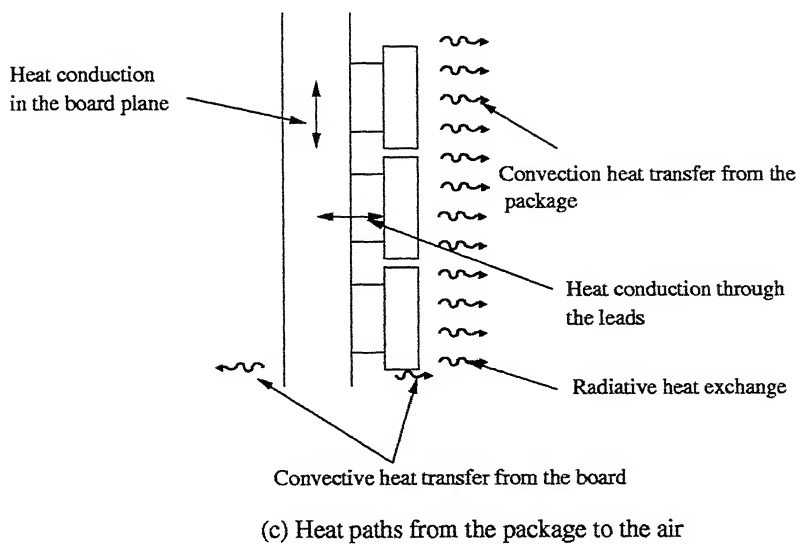
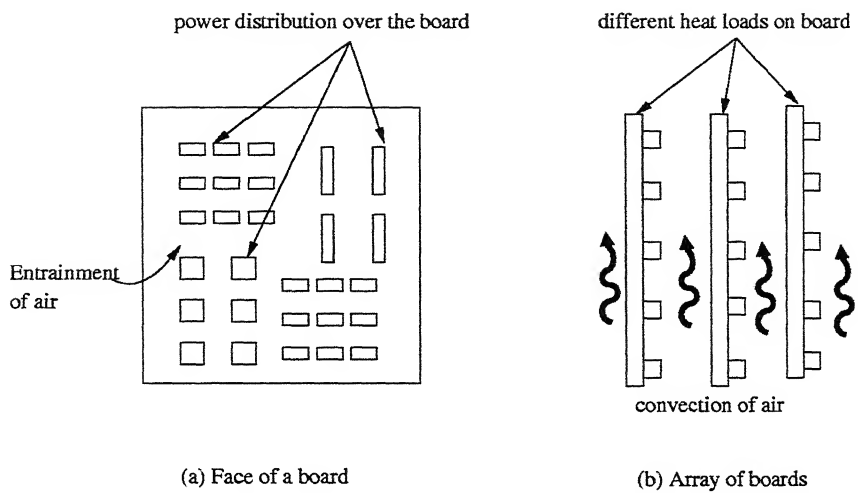


Figure 1.2 Factors Affecting Natural Convection Cooled PCB's.

they permit more heat to be removed. However, turbulent flow will usually result in a greater pressure drop, through the system, which requires that larger pumps and fans and more power be used to overcome the added resistance.

1.5 Electronic Cooling by Mixed Convection

The effect of gravity field is always present in forced flow heat transfer as a result of the buoyancy forces connected with the temperature differences. Forced flows in which this buoyancy driven flow also affects the main flow is called mixed convection. Heat transfer in mixed convection can be significantly different from its value in both natural and pure forced convection. The heat transfer in the case of mixed convection depends on the duct geometry, the orientation of the duct, and whether the flow is fully developed or developing.

All these efforts lead to an objective, i.e., to maintain the constant component temperature, which should be in between 65°C and 85°C . Thermal control schemes to remove the heat from individual devices and systems include the traditional means of free and forced gaseous and liquid convection as well as conduction and radiation or combination thereof. Electronic cooling is further classified into two broad classes viz. direct cooling and indirect cooling. Direct cooling methods are capable of attaining high heat flux levels, but they present problems with contamination and are extremely expensive. In indirect cooling heat is removed firstly by primary coolant and then it is transferred to secondary coolant like air. The flow chart given in figure 1.3 shows different steps to be taken by a thermal designer to ensure a perfect design.

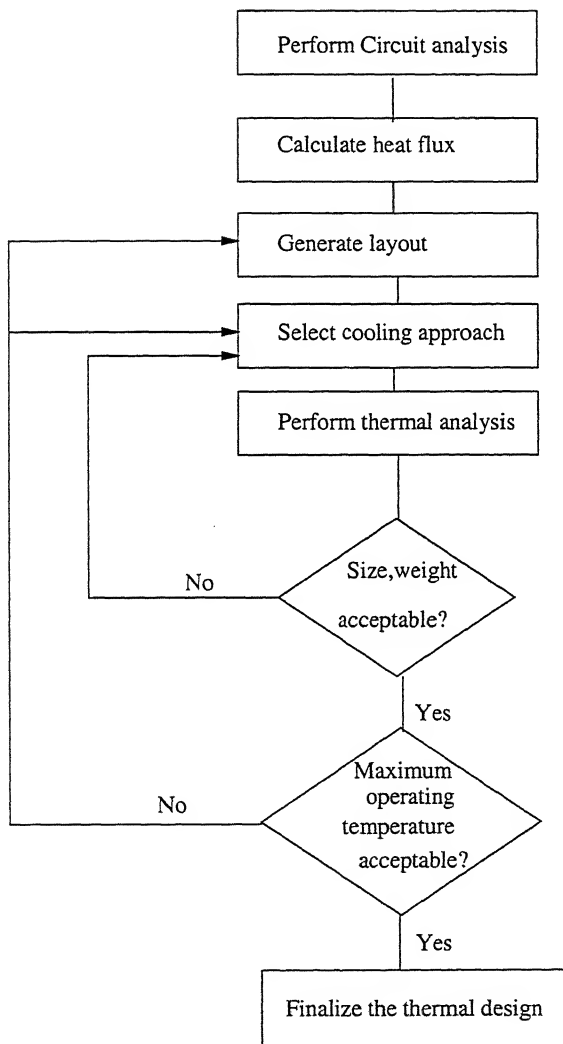


Figure 1.3 Flow Chart to be Followed by a Thermal Designer

So, in order to design a better cooling systems for electronic equipments, following four aspects are to be taken into account: -

- 1.*Fixed quantities*: Energy dissipated per component, number of components, basic geometry, configuration of the circuitry, energy input per component etc.
- 2.*Requirements*: Desired temperature level of electronic components such as chips. There should be no concentration of thermal or hot spots.
- 3.*Constraints*: Material temperature limitations, size and geometry limitations, fluid in contact must be electrically insulating, limitations on fluid flow rate from pressure considerations.
- 4.*Design Variables*: Cooling fluids; mode of cooling including possibility of phase change, particularly boiling; inlet temperature of fluid; velocity of fluid or flow rate; fan characteristics; fins for enhanced cooling; and dimensions.

One more quantity of interest is the pressure head needed to maintain the flow to select an appropriate blower or fan. The estimate of overall energy removed out of the system is must. In the event of failure of efforts to eliminate hot spots through mentioned enhancement techniques, one has to opt for special local arrangements such as heat pipes, heat sink, impinging jet of cold fluids, localized boiling etc.

1.6 Scope of Present Work

The objectives of the present work are-

- To develop a test rig which simulate the PCBs in an electronic system.
- To conduct experiments to find the effects of various parameters.

The performance of the PCBs depends upon the spacing between them and the pressure difference across the channel. The test rig developed in the present study attempts to incorporate the effects of all these factors.

Chapter 2

LITERATURE SURVEY

2.1 Introduction

This chapter contains the summary of the analytical, numerical and experimental work reported in the literature. This survey, not only facilitates the improvement of existing schemes, but also provides a base for newer techniques in this field.

Till now, the works in the field of electronic cooling can be broadly classified into following categories:

- (A) Natural convection cooling
- (B) Mixed convection cooling
- (C) Forced convection cooling
- (D) Boiling and immersion cooling
- (E) Miscellaneous cooling

2.2 Natural Convection Cooling

Manca et al. [1] did an experimental investigation of natural convection between horizontal heated, parallel plates in air by visualizing the flow and measuring the air temperature. Grashoff number, based on the plate spacing, varied in the 1.22×10^5 –

1.06×10^6 range. Flow patterns and probable onset of secondary motions were observed for three heating modes:

- (1) Both plates heated
- (2) Upper plate heated and lower unheated, and
- (3) Upper plate unheated and lower plate heated

The main flow patterns resembled a C shape (C loop) for all modes. In fact, the flow penetrated inside the cavity close to the leading edge of the lower plate and exited from the upper part by reversing its motion between the plates. When the lower plate was heated, flow visualization showed that secondary flows were added to the C loop main flow. Such secondary structures changed into longitudinal vortices and in the upper region of the open-ended cavity a chaotic motion was detected. The existence of these structures was confirmed by measurements of instantaneous temperature values. They showed that the greater the Grashoff number the more chaotic was the flow in the C loop when the lower plate was heated and the upper plate was not.

Sezai et al. [2] studied a steady, natural convection from a discrete flush-mounted rectangular heat source on the bottom of a horizontal enclosure. Using multi-grid technique they solved three-dimensional form of Navier-Stokes equations. Rayleigh number based on the enclosure height was varied from 10^3 until unstable flow was predicted for a fixed Prandtl number of 0.71. Aspect ratio of the source was varied until it fully covered the entire width of the bottom plate. The enclosure was cooled from above and insulated from the bottom. Effect of vertical boundary conditions on the rate of heat transfer from the heat source was studied. It was found that the rate of heat transfer was not so sensitive to the vertical wall boundary conditions. The limit of maximum Rayleigh

number to obtain a convergent solution decreased as aspect ratio of the source was increased. The variation of Nusselt number as a function of Rayleigh number and aspect ratio of the source was also reported.

Lee et al. [3] investigated numerically the laminar natural convection heat and mass transfer in open vertical rectangular ducts with uniform wall temperature/ uniform wall concentration or uniform heat fluxes/uniform mass flux boundary conditions. For simplifications following assumptions were made:

- (1) The flow was assumed to be laminar, steady, boundary-layer type and with constant properties except the density variation of the buoyancy term in the Z-momentum equation.
- (2) The Boussinesq approximation was used to characterize the buoyancy effects.
- (3) The viscous dissipation effect was negligible.
- (4) The surface normal velocity was ignored due to the small temperature and concentration differences.

The vorticity-velocity formulation was applied to solve the coupled momentum, energy and concentration equations. The Q , Nu and Sh were found to increase with buoyancy ratio. The characteristics of natural convection in vertical rectangular ducts would approach those of two dimensional vertical plate ducts as aspect ratio γ was greater than 31.

Liu et al. [4] did a numerical analysis of optimum spacing problems for three heated elements mounted on a vertical substrate using an operator –splitting time stepping finite element method. The governing equations were the conservation of mass, momentum and

energy for the enclosure fluid and the energy equations for the solid phases. It was obtained that

1. By changing the space among chips, the temperature gradient from the bottom to the top chips could apparently be reduced, and consequently the maximum temperature could be reduced.
2. From the thermal point of view, the conventional equi-spaced arrangement was not an optimum option and should be avoided.
3. With the optimum spacing arrangement, the relative temperature drop was about 10%.

Mendez et al. [5] studied the steady state heat transfer characteristics of a thin vertical strip with internal heat generation. The non-dimensional temperature distribution in the strip was obtained as a function of the following parameters.

1. The intensity and distribution of the internal heat sources
2. The aspect ratio of the strip
3. The longitudinal heat conductance of the strip
4. The Prandtl number of the fluid. Both the thermally thin and the thick wall approximations were considered. The total thermal energy or averaged temperature of the strip was found to decrease as the influence of the longitudinal heat conduction effects in the strip decreased in the thermally thin wall regime. After reaching a minimum, it increased again in the thermally thick wall regime.

2.3 Mixed Convection Cooling

Chen et al. [6] investigated the linear stability analysis of mixed convection in a differentially heated vertical channel for Prandtl number values of 0.7, 7, 100 and 1000.

The viscous flow investigated in this paper was the mixed convection, which was driven by an external pressure gradient and also by a buoyancy force, between two parallel long vertical plates separated by a distance. The gravitational force was aligned in the negative x-direction. There was a fixed temperature difference, produced by maintaining the two vertical walls at different temperatures of T_1 and T_2 respectively. It was found that both the Prandtl number and the Reynolds number were very important parameters in determining the critical Grashoff number Gr_c , critical wave number α_c , wave speed C_r and instability mechanism for higher Prandtl numbers. For lower Prandtl numbers, the effects of the Prandtl number and the Reynolds number were relatively small. The most significant finding was that the local minimum wave numbers can be as high as 8 for $Pr=1000$, which was substantially higher than those found before for other heated flows. In general, for mixed convection channel flows, the instability characteristics of differentially heated flows were found to be substantially different from those of uniformly heated flows.

Barletta et al. [7] investigated mixed convection of a power-law fluid in a vertical annular duct in a regime of laminar and fully developed flow. Uniform and unequal temperatures were prescribed on the inner and outer boundary walls. The momentum balance and the energy balance equations as well as the viscous stress constitutive equation were solved analytically in order to obtain the velocity fields, the viscous stress field and the temperature field. Analysis of the cases was done for

1. Mixed convection of a Newtonian fluid
2. Forced convection of a power-law fluid

In the first case, it was shown that the condition for the onset of reversed flow implied the existence of a threshold value for $|\Lambda = \frac{Gr}{Re}|$ which depended on $\gamma = (R1/R2 \text{ ratio of inner to outer radii})$. When these threshold values were exceeded, flow reversal occurred next to the inner boundary wall. In case of mixed convection for power-law fluids, the flow reversal conditions were investigated. As for Newtonian fluids, flow reversal occurred when threshold values of $|\Lambda|$ were exceeded. These threshold values depended both on γ and on m (=inverse of power law index) and for a fixed value of γ , were increasing function of m .

Barletta et al. [8] analyzed the fully developed and laminar convection with viscous dissipation in a vertical channel such that one wall was subjected to a prescribed and uniform heat flux while the other wall was kept at a uniform temperature. The velocity field and the temperature field were evaluated by means of perturbation expansion with respect to a buoyancy parameter, i.e. the ratio between Grashoff number and the Reynolds number. The following results were observed:

1. The effect of buoyancy was more apparent for upward flow than for downward flow.
2. In the case of downward flow, the absolute values of Nusselt numbers on both walls and the friction factor on the boundary with a prescribed temperature were increased by buoyancy. The opposite occurred in the case of upward flow.
3. Flow reversal next to boundary with a prescribed temperature occurred for upward flow with a sufficiently high value of (Gr/Re) and for positive values of Br_q (heat flux Brinkman number).

Moukallaed et al. [9] numerically studied the mixed convection heat transfer in channels with a heated curved surface bounded by a vertical adiabatic wall. Two cases

were considered, in the first case the flow experienced a convex curvature on an increasing cross-sectional flow area (adverse pressure gradient), while in the second case, the flow experienced a concave curvature with a decreasing flow cross-section (favorable pressure gradient). Governing equations were conservation of mass, momentum and energy. Flow was considered to be steady, laminar and two-dimensional. The control volume approach was adopted to solve numerically the coupled system of equations governing the flow and temperature fields numerically. For convex-entry channel it was observed that for low (Gr/Re^2) , the Nusselt number reached a minimum near the onset of flow separation along the heated wall of the convex-entry channel and then decreased toward the channel exit. The effect of increasing Prandtl number on the total heat transfer was considerably greater than the effect of increasing (Gr/Re^2) . For concave –entry channels, flow separation was not encountered. The decreasing cross sectional area combined with buoyancy increased the channel velocities and the near wall gradients. Therefore surface heat transfer rates were considerably greater than in convex-entry channel. The overall heat transfer in a concave-entry channel was always greater than a straight channel of equal height. When compared to a straight channel of equal heated surface area, a critical (Gr/Re^2) value existed, below which heat transfer enhancement was obtained with concave-entry channels.

Yadav and Kant et al. [10] developed a theoretical model to numerically simulate mixed convection cooling in a stack of vertical heated plates used as PCB's. For the given spacing between the plates, they estimated the maximum amount of heat that could possibly be transferred to the coolant at a certain static pressure difference between the top and bottom of the stack and also the maximum possible heat flux from the surface

being cooled. It was shown that the need for the optimum spacing between the plates became more important when the driving static pressure reached a relatively high level. An empirical equation was suggested for predicting the heat flux corresponding to optimum plate spacing for a given static pressure.

Yao et al. [31] analytically studied fluid flow and heat transfer in the entry region of a heated vertical channel. The entrance of the channel was connected to a chamber so that a uniformly distributed inlet velocity profile resulted, due to the rapid contraction of the fluid passage between the chamber and the channel. Both constant temperature and constant heat flux conditions along the channel wall were studied. The solution was obtained by treating the natural-convection effect as a perturbation on the solution of the entry flow in an isothermal channel. Different axial length scales were revealed by the analytical solution. These scales distinguished the regions of different convective mechanisms that a developing flow had to pass through before reaching its fully developed state. The solution also indicated that natural convection eventually became the dominant heat transfer mode if $Gr > Re$ for constant wall temperature, and $Gr^2 > Re$ for constant wall heat flux. If natural convection was a dominant mode, the evidence suggested that moving periodic and recirculating cells were generated.

2.4 Forced Convection Cooling

Argento et al. [11] studied the thermal design of a forced convection air-cooled chassis, using an integrated experimental and computational approach. Finite volume CFD/CHT code FLOTHERM was used for the computational modeling. Improvement in flow pattern near heated areas was attempted by considering sixteen different baffle

designs. The best thermal performance was obtained for a plenum configuration consisting of three varying sized baffles. Implementation of this modification into the experimental chassis provided surface temperature reduction by as much as 56%. The effectiveness of the changes in configuration recommended based on the computational study was also experimentally verified.

Coprland et al. [12] studied forced convection from rectangular arrays of electronic components. Effects of channel height, planar spacing, component row number, and approach velocity were assessed. Correlations for the temperature rise of a component due to its own power and due to heating by upstream modules were presented. The space between the row and columns of modules was varied from near zero to about one module length. Channel height ranged from about two to five velocity ranging from 0.5 to 5.5m/s. Corresponding to module length Reynolds number ranged from 1000 to 11000. The heat transfer coefficient varied from 25 to 75W/m²-K. It was observed that heat transfer rate was principally a function of planar spacing and approach velocity, and a weaker function of row number and channel height. The temperature rise of components downstream of a heated component exhibited similar, but stronger dependence on velocity and channel height and the same dependence on row number. The effect of velocity was weaker on the densest configuration than on the two sparser spacing.

Leung et al. [13] obtained the systematic computational results for forced convective cooling of the horizontal PCB assembly. To enhance the calculation accuracy, a second-order upwind scheme was adopted and a sufficient mesh density was arranged near the wall region. The considered assembly consisted of a channel formed by two parallel plates. The upper plate was thermally insulated, whereas the bottom plate was attached

with uniformly spaced identical electrically heated square ribs, perpendicular to the mean airflow. The bottom plate was used to simulate the PCB, and the ribs with heat generation were used to simulate the electronic components. The dependence of flow and temperature fields on Reynolds number, obstacle sizes, and the separation between two obstacles was documented and the results showed that these parameters had a significant effect on the flow and temperature fields.

Young et al. [14] numerically simulated the forced convective, incompressible flow in a channel with an array of heated obstacles attached to one wall. The flow was assumed to be Newtonian. Buoyancy effects were assumed to be negligible, as were those of viscous heat dissipation. Three values of Nusselt numbers were emphasized in this systematic analysis: local distributions along the obstacle exposed faces, mean values for individual faces, and overall obstacle mean values. This study observed the effects of variations in the obstacle height, width, spacing, and number, along with the obstacle thermal conductivity, which was varied between values typical of electronic component material. Smaller, widely spaced obstacles were found to more effectively transfer thermal energy into the fluid, reducing their temperatures. Narrow gaps between tall obstacles were found to allow upstream thermal transport by the cavity vortices through reduced cavity-core flow interaction, in some cases actually heating the upstream obstacles. Differences between surface flux and volumetric heating manifested themselves in the isotherms within the obstacles with only small changes in Nusselt numbers. Large values of the solid thermal conductivity effectively isothermalized the obstacles regardless of heating method or geometry.

Tso et al. [15] measured convective heat transfer from a linear array of flush-mounted heat source in a vertical up-flow channel. Water was used to simulate the dielectric fluid. The dimensions of the simulated chips were held constant while the height of the channel was varied. The experiments were conducted in a closed-loop liquid cooling flow facility, with a vertical up-flow, in a plexiglas test section. The first chip was located 680mm downstream of the channel inlet, providing a minimum hydrodynamic entry length of 50 hydraulic diameters. Channel height was varied over values of 0.5, 0.7, 1.0 times the heat source length. The heat flux was set at the three values of 5W/cm^2 , 10W/cm^2 and 20W/cm^2 . Reynolds number based on the heat source length ranged from 6×10^2 to 8×10^4 . The results obtained agree well with results for air-cooling of heat sources of similar geometry when Pecelt numbers were used to correlate the data in laminar flow and Nusselt numbers were normalized against the Prandtl number in turbulent flow. This suggested that data from air-cooling might be used to predict the heat transfer characteristics of liquid cooling for similar geometry if the Prandtl number scaling was considered.

2.5 Immersion Cooling

Liquid cooling of microelectronic component succeed in removing higher heat fluxes in comparison to forced air-cooling or indirectly water-cooling. The liquids used are dielectric called as Fluorinates. Dehghan et al. [16] studied the natural convection immersion cooling of two heat sources in a series of parallel interacting cavities filled with FC-72. Increasing Ra^* (modified Rayleigh number) led to a stronger convective flow inside the cavities for all values of kr (thermal conductivity ratio of wall and fluid). Thin

thermal and velocity boundary layers are found along both faces of the vertical walls and the cold fluid occupied the rest of the cavity. For low values of k_r (e.g. bakelite substrate) the flow and thermal fields were asymmetric whilst for higher conductivity substrates (e.g. alumina-ceramic), symmetrical flow patterns were observed.

2.6 Miscellaneous Works

Fedorov et al. [17] developed a three-dimensional model to investigate flow and conjugate heat-transfer in the micro-channel based heat sink for electronic packaging applications. The incompressible laminar Navier-Stokes equations of motion were employed as the governing conservation equations, which were numerically solved using the generalized single-equation framework for solving conjugate problems. Theoretical analysis and experimental data strongly indicated that the forced convection water-cooled micro-channel heat sink had a superior potential for application in thermal management of the electronic packages. The heat sink was compact and was capable of dissipating a significant thermal load (heat fluxes of the order $100\text{W}/\text{cm}^2$) with a relatively small increase in the package temperature (less than 20°C) if operated at the Reynolds number above 150.

Lee et al. [18] did a comparative investigation of jet impingement and micro-channel cooling. The major concern of this study was to evaluate attainable maximum heat flux by jet impingement. It was revealed that the micro-channel cooling was preferable for a target dimension smaller than $0.07\text{cm}\times 0.67\text{cm}$, while the jet impingement was found to be comparable or better than the micro-channel cooling for a larger target plate if a proper treatment was applied for the spent flow after the impingement. The jet

impingement cooling usually required a very large coolant flow rate with a relatively small pressure drop, while the micro-channel cooling was subjected to a larger pressure drop even for a relatively small coolant flow rate. Subsequently, a constant pressure drop condition would be preferable for the jet impingement while a constant coolant flow rate condition would be advantageous for the micro-channel cooling.

Vafai et al. [19] proposed a new concept for a two-layered micro-channel heat sink with counter flow arrangement for cooling of the electronic components. The thermal performance and the temperature distribution for these types of micro-channels were analyzed and a procedure for optimizing the geometrical design parameters was presented. While the power supply system of the two-layered design was not significantly more complicated than the one-layered design, the stream wise temperature rise on the base surface was found to be substantially reduced compared to that of the one-layered heat sink. At the same time, the pressure drop required for the two-layered heat sink was found to be substantially smaller than that of the one –layered heat sink. The results demonstrated that the two-layered micro-channel heat sink design was a substantially improvement over the conventional one-layered micro-channel heat sink.

Kim et al. [20] obtained the analytical solutions for temperature distributions in the micro-channel heat sink using both one-equation and two-equation models for heat transfer. The problem under consideration was forced convective flow through a micro-channel. The bottom surface was uniformly heated and the top surface was insulated. A coolant passed through the micro channel and takes heat away from a heat-dissipating component attached to the micro-channel heat sink. To analyze the problem, the flow was assumed to be laminar and both hydro dynamically and thermally fully developed. All

thermo-physical properties were assumed to be constant. To analyze fluid flow and heat transfer through the micro-channel heat sink, the Brinkman-extended Darcy equation and volume-averaged energy equation for the solid and fluid phases were solved. From the analytical solutions, variables of engineering importance were identified as the Darcy number (D_a) and the effective thermal conductivity ratio (C). As either D_a decreased or C increased, the fluid temperature approached the solid temperature, in which case the above assumption and the one-equation model would be appropriate. In addition, as either one of D_a and C decreased, the overall Nusselt number of the micro-channel heat sink Nu_∞ was shown to increase to an asymptotic value.

Wolfersdorf et al [21] adopted a shape optimization method for convective cooling channels within a two-dimensional heat conduction region. This method combined genetic algorithms with a point heat sink approach that was used to model the heat removal of the cooling channels during the optimization process.

Greiner et al. [22] did a direct numerical simulation of three-dimensional flow and augmented convective heat transfer in a traversal grooved channel for the Reynolds number range of 140 to 2000. These calculations employed the spectral element technique. Multiple flow transitions were reported as the Reynolds number increased from steady 2-D flow through broad-banded unsteady 3-D mixing. At $Re=325$ the flow was steady and two-dimensional but it exhibited a series of transitions with increasing Reynolds number. At $Re=350$, it exhibited 2-D traveling waves. For $Re=483$, the flow was observed to have regular variations in the cross-stream direction and to be time periodic. At $Re=748$, the flow exhibited irregularities in the direction normal to flow.

Finally for $Re=1530$ the three-dimensional flow structure was very irregular and a broad band of flow frequencies was observed.

Kato et al. [23] conducted a theoretical study of turbulent channel flows in order to investigate the relationship between the heat transfer enhancement and the increase in drag by rough surfaces using time spaced averaged momentum and energy equations. A fully developed turbulent flow in a two-dimensional channel with a constant heat flux from the wall was considered in this study. Three-dimensional arbitrary-shaped roughness elements were placed on the bottom surface of the channel. It was assumed that the heat flux from the bottom surface of the channel was the same irrespective of the surface roughness. The flow rate was also assumed to be same for rough and smooth surface channels. It was found that it would be difficult for the heat-transfer efficiency of rough surfaces to become greater than unity when the molecular Prandtl number of working fluid was smaller than the turbulent Prandtl number. This was due to the fact that the contribution of roughness surfaces to the drag increases was usually greater than that to the heat-transfer enhancement. When the molecular Prandtl number was greater than the turbulent Prandtl number, however the heat-transfer efficiency may become greater than unity, since the increase in eddy viscosity over rough surfaces could have a greater effect on the heat transfer than the pressure loss. Some of the drag-reducing riblet-surfaces were known to have high heat-transfer efficiency. When the thermal boundary layer over a riblet surface was thinner than the momentum boundary layer; the effect of roughness elements on heat-transfer enhancement became significant even if the riblet size was small.

Chin et al. [24] made a comparison of the solution between the parabolic and the full elliptic models to demonstrate the validity and relative performance of the model for predicting three-dimensional flow separation in a vertical, asymmetrically heated, rectangular duct. The flow was assumed to be steady, laminar and incompressible; fluid properties were constant except the density variation appearing in the buoyancy term of the momentum equation for the axial direction; and the density variation was defined by the Boussineq's approximation. It was concluded that parabolic model was an efficient alternative, which may give fast but accurate solutions for predicting 3D flow separation.

Choi et al. [25] conducted numerical study to determine the effects of the Reynolds number and width ratio D_c/D_d (defined as the ratio of the combining headed width to the dividing header width) on the coolant distribution in a parallel flow manifold used in liquid cooling modules for electronic packaging. Because the coolant flow in electronic packaging was laminar, low inlet Reynolds numbers of 5, 50 and 250 were used. Two-dimensional, steady flow with a uniform inlet velocity profile was assumed. It was observed that flow distribution in a manifold was highly dependent on the Reynolds number. When the Reynolds number was increased, the flow rates in channel near the entrance decreased i.e., as the flow rate is increased, the dimensional pressure ($P/\rho V_{in}^2$) decreased. Of the four width ratios (0.5, 1.0, 2.0 and 4.0) the case of $D_c/D_d=4.0$ produced the maximum channel flow rate.

Jubran et al. [26] made an experiment to study the effects of various designs of secondary air injection hole arrangements on the heat transfer coefficient and the pressure drop characteristics of an array of rectangular modules at different values of free-stream. Reynolds numbers varied in the range 8×10^3 to 2×10^4 . The set up consisted mainly of a

suction type wind tunnel with maximum flow rate of $0.24\text{m}^3/\text{s}$. The main body of the test section was a channel-like box 2m in length \times 0.33m wide \times 0.04m high. At the air intake side of the wind tunnel a bell mouth is attached, and a flow straightener was placed at the front and at the trailing edge of the wind tunnel test section with a gradient contraction, which is connected to a circular cross-section pipe of the fan. The arrangement used in either one staggered row of the simple holes or one row of compound injection holes. The pitch distance between the injection holes, as well as the injection angles were varied in both the stream wise and span wise directions (see figure 2.1). It was concluded that the reductions in the injection angles of the secondary air tend to enhance the heat transfer from the electronic modules for both the compound angle and simple angle injection holes. The pressure drop coefficient ratio across the electronic modules was essentially a weak function of the blowing rates ratio that gave the highest heat transfer enhancement was dependent on the injection angle of the hole and P/D (P the distance between injection holes and D diameter of the injection cylinders or holes).

Fitzgerald et al. [27] studied experimentally the flow field of an axi-symmetric confined and submerged turbulent jet impinging on a flat plate using laser-doppler velocimetry. These jets were used in turbine-blade cooling, paper drying and electronic packaging. A jet of FC-77 (a per fluorinated; dielectric liquid with $Pr=25.3$, $\rho=178\text{kg}/\text{m}^3$ and $\nu=0.86\times 10^{-6}\text{ m}^2/\text{s}$ at 20°C) issued at 20°C from the nozzle into a tank of stagnant fluid. Nozzle diameters of 6.35 and 3.18mm were used. The location of the center of the toroid moved radially outward, both with an increase in Reynolds number and with an increase in nozzle-to-target plate spacing. The center of the toroid moved nearer to the target plate with an increase in Reynolds number. An increase in the nozzle-to-target

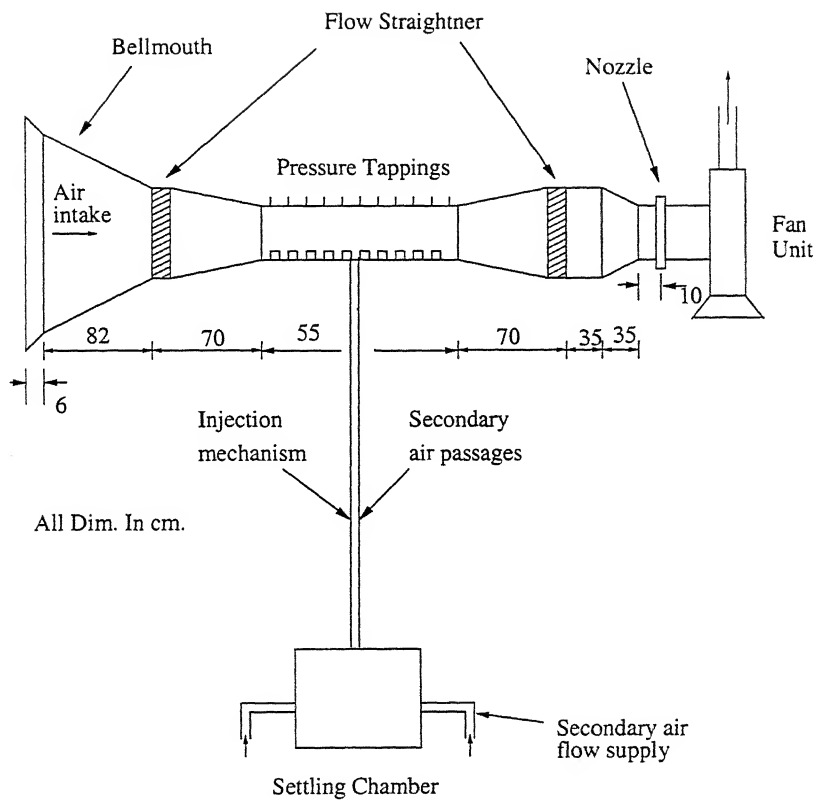


Fig 2.1 Schematic Diagram of the Experimental Set-Up

plate spacing reduced the magnitudes of radial velocities as well as the peak turbulence intensities in the flow field. Increasing the nozzle diameter resulted in a decrease in peak radial velocity, but an increase in peak turbulence levels.

Parneix et al. [28] numerically studied the problem of cooling of a heated plate by an axis-symmetric isothermal fully developed turbulent jet. The axis-symmetric, incompressible, Reynolds averaged Navier Stokes equations were solved in conjunction with the k - ϵ and ν^2 transport equations. The computations carried out herein showed that predictions by the normal-velocity relaxation model agreed well with the experiments. The k - ϵ model did not properly represent the flow features, highly over-predicted the rate of heat transfer and yielded physically unrealistic behavior.

Huang et al. [29] performed heat transfer and flow visualization experiments to investigate and compare the heat transfer performance of new swirling jet designs with that of a conventional impinging jet having the same diameter at the same conditions. Swirling impinging jets employed a 25.4mm long solid insert at the exit of tube to divert the air flow through four narrow channels along the surface of the insert, with the desired swirl angle (15° , 30° and 45°). Flow field visualization experiments employed three flow visualization techniques. Smoke flow; smoke wires and water jet seeded with tiny air bubbles used as tracers. The smoke flow technique showed that the flow field between the exit of the jet housing tube and impinged surface, while the smoke wires technique gave clear images showing details of the flow field at and close to the impinged surface. It was observed that swirling impinging jet induced markedly higher local and surface average Nusselt number values and improved radial uniformity of heat transfer on the

impinging surface compared to conventional impinging jet. Nusselt number for swirling impinging jets was higher than for conventional impinging jet at intermediate jet spacing.

Voke et al. [30] studied computationally the impingement of a thermally inhomogeneous turbulent jet on a solid plate, using large-eddy simulation. The case of a plane channel into an enclosed pool and impinging normally on perspex plate 1.8 jet-widths was investigated. It was shown that the dynamics of the turbulence in this particular geometry resulted in the temperature variations at the plate surface having very high lateral correlation, so that lateral conduction of heat within the plate failed to have any significant effect on the transmission of thermal fluctuations from the fluid into the plate.

Chapter 3

PROBLEM FORMULATION AND EXPERIMENTAL SET-UP REQUIREMENTS

3.1 Introduction

An electronic device consists of a large number of heat-generating sources mounted on insulated plates called printed circuit boards (PCB's). The heat generating capacity of each PCB is different from the others hence, the surface temperature. For proper functioning of an electronic component its surface temperature should be lower than that specified by manufacturer or by material limitations. For most of the electronic devices these maximum temperature limit lie in between 85°C and 100°C . For cooling of these electronic components, many investigations have been done in the field of natural convection and forced convection but less in the field of mixed convection. As natural and forced convection have their advantages, they have some disadvantages too. Mixed convection inherit the merits of both heat transfer mechanisms and hence it has several desired features:

1. Creates lesser noise than forced convection for the same amount of heat removal
2. Needs lesser fan power than forced convection
3. Able to work for a longer duration when there is a sudden power failure

3.2 Experimental Requirements

In order to conduct experimental study on the cooling mechanism inside various electronic equipment and devices one has to take into account many extremely flexible possibilities or requirements like-

1. PCBs could have a variety of dimensions;
2. PCB's could have a number of possible arrangements;
3. Number of orientations possible for a single PCB relative to other PCBs and also entire PCB stack/assembly could be oriented in different way;
4. Varieties of possible mountings or arrangements for electronic chips are possible, each chip having a different surface temperature;
5. Cooling could be done either using air as working fluid or any other fluids
6. The cooling process may be through submerged boiling heat transfer, conduction to surrounding bodies, natural convection, forced convection, mixed convection etc;
7. The unit driving the working fluid or static pressure creating device can be located at different positions inside or outside the cabinet;
8. It is likely that the electronic devices are not stationary at all during their operation for example, those working inside airplanes, rockets, satellites, marine vehicles etc. In such cases different inertial forces act on the working fluid, affecting its path of motion.

On the other hand we cannot neglect some of the highly restrictive conditions like;

1. The semi-conductor materials of which the electronic devices are made are extremely temperature sensitive. This results in the requirement that the individual electronic component must work under a specified thermal condition.

2. Even if a single component (like chip) on the PCB generates more heat compared to others or demands to be kept below the temperature range needed by the others, it can alter the thermal environment in which the PCB or the entire device has to be placed;
3. Coolant or the working fluid must possess specified thermodynamic properties within the operating temperature range of the device or requirements;
4. Coolant or the working fluid must have certain electrical properties under the given thermal conditions inside the device or equipment;
5. Driving fan or unit must be located at the place from where the acoustic electromagnetic disturbances shall have minimum effect (even if it has electromagnetic shields) on highly sensitive electronic components mounted inside;
6. Movement of working fluid should be within certain limits. It should not create large turbulence inside the cabinet, which may lead to mechanical or electrical damages;
7. There should be a provision for air filters, resulting in pressure losses. Fine dust particles that are difficult to trap can cause micro scratches on the delicate components surface; choke the micro passages for coolant entry over a period of time, which can lead to malfunctioning of the entire equipment or device.

Therefore, some of the sub-objectives of this work are-

1. To select the commonly used dimension of a (typical) PCB;
2. To select the temperature distribution over the PCB;
3. To select a range of heat generation rate or heat flux from the PCB surfaces;
4. To select a most acceptable arrangement and orientation of PCBs; and
5. To select a working fluid, its temperature range, maximum allowable velocity and other physical, thermodynamic & electrical properties and conditions.

- i. To fabricate the PCBs with chosen surface conditions. If possible otherwise to model it in some other simpler form;
7. To design and fabricate a channel through which working fluid can flow and some mechanism with which it is possible to orient the PCBs in several ways;
8. To design and fabricate a coolant-driving unit with a range of static pressure developing capacity usually required in electronic equipment;
9. To choose the shape and dimensions of channel entry for wide range of coolant discharge;
10. To develop a suitable method or mechanism for the control and measurement of heat flux through PCBs without disturbing the flow pattern over their surfaces;
11. Also, to develop a method to find overall heat loss from the PCBs individually and as a whole assembly; and
12. To conduct the experiment where PCBs or model PCBs are subjected to natural and mixed convection cooling and to study:
 - Effect of spacing on the cooling rate;
 - Effect of (cooling fluid) discharge on the cooling rate;
 - Find the range of spacing, discharge and other relevant parameters within which the cooling is most effective;
 - Obtain overall power required for cooling (i.e. by driving unit) and to calculate the efficiency and estimate the efficiency of the cooling effort;
 - Present the experimental data in a manner, which is relevant for thermal designing of electronic equipment or devices.

Chapter 4

MODELING AND APPARATUS DESIGN

4.1 Introduction

As mentioned previously, for proper functioning of an electronic component the surface temperature should not exceed the limiting value that is generally in between 85°C and 100°C for most of the components. In reality, the surface temperature at different locations on a PCB is not same, which is due to the non-uniform heat generation and different flow patterns at each and every location. The typical arrangement of any electronic system is shown in figures 4.1a and 4.1b. It is extremely difficult to deal with the PCBs as such. To deal with such a system, two kinds of models are suggested namely an isoflux or uniform flux model and the other one is the isothermal model. In the present work, a vertical plate with uniform heat flux is simulated as a PCB and the channel between two vertical heated plates as the channel between the two PCBs. Mixed convection heat transfer will take place in the channel as the buoyancy driven flow has significant effect on the main flow that is caused by pressure difference across the channel. Flow was assumed to be one dimensional, steady, incompressible and laminar. Boussinesq approximation was assumed.

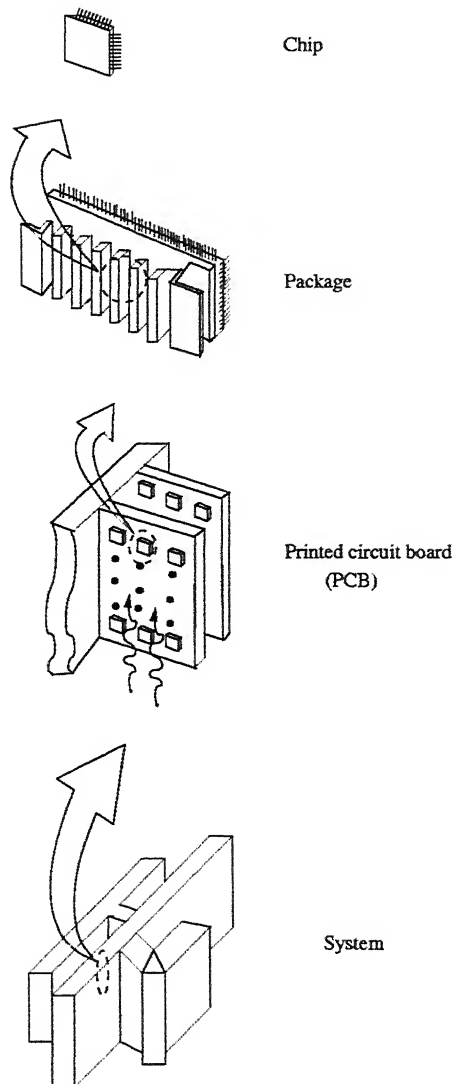


Figure 4.1a Structural Levels of An Electronic Computer

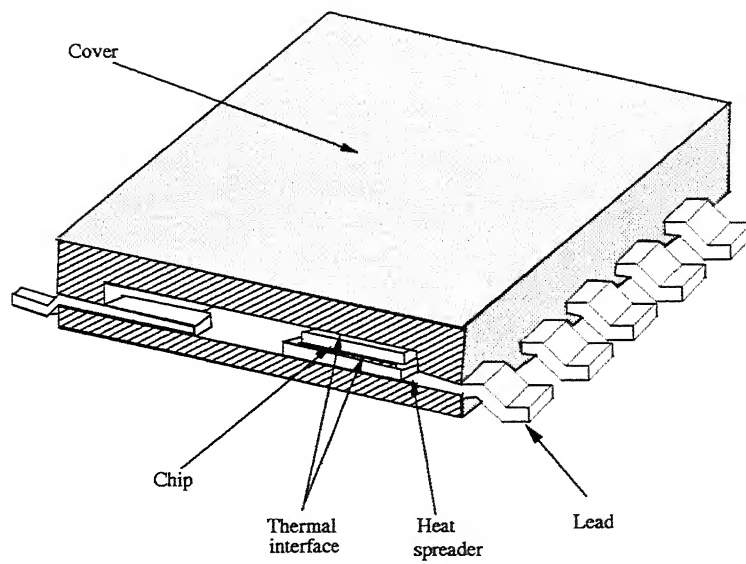


Figure 4.1b Primary Components of a Package.

1.2 Test Rig Design and Construction

1.2.1 General Considerations

The type and construction of the test rig was dictated by the objectives of the experiment. After the obvious and paramount necessity of safety considerations for the personnel and the facilities come sufficient accuracy, accessibility, and maintenance. The model was usually so placed that accessibility was at a premium and repair could be done easily. All these factors demanded that changes be as simple as possible and the model with all its parts and additions be thoroughly tested outside the short tunnel before tests were commenced. Provisions for rapid configuration changes were very important. Model design and construction had traditionally been a relatively long and tedious process. It was often the pacing activity that determined whether an appropriate experiment could be timely and cost effective. Planning was another major factor, which decided whether model would be made timely or not. Fig. 4.2a shows the process diagram for experiment planning and execution. A block diagram representation of experimental test rig is shown in Fig.4.2b. The elements of the input vectors were variables such as spacing between plates, pressure differential across channel. The elements of the controllable vectors were variables such as set-up size, tunnel size, material used in the test rig. The elements of the output vector were heat flux, plate temperatures, flow rates etc. Elements of the uncontrollable factor vector included such variables as turbulence level of the incoming stream, relative humidity and instrument inherent errors or uncertainties. Figure 4.3 shows the schematic diagram of the test rig designed to study the mixed convection heat transfer in PCB.

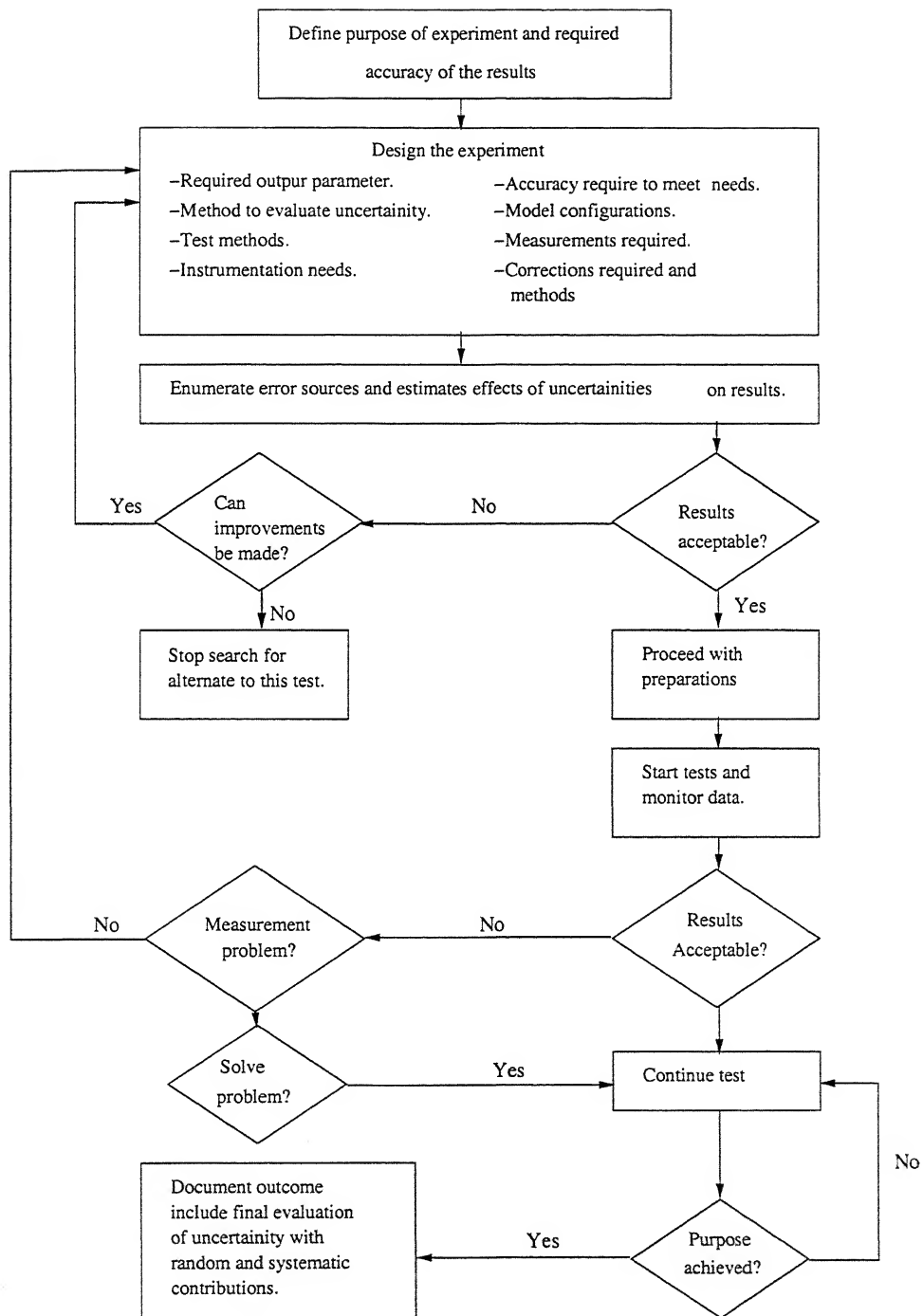


Figure 4.2a Experimental Planning and Execution Process Diagram.

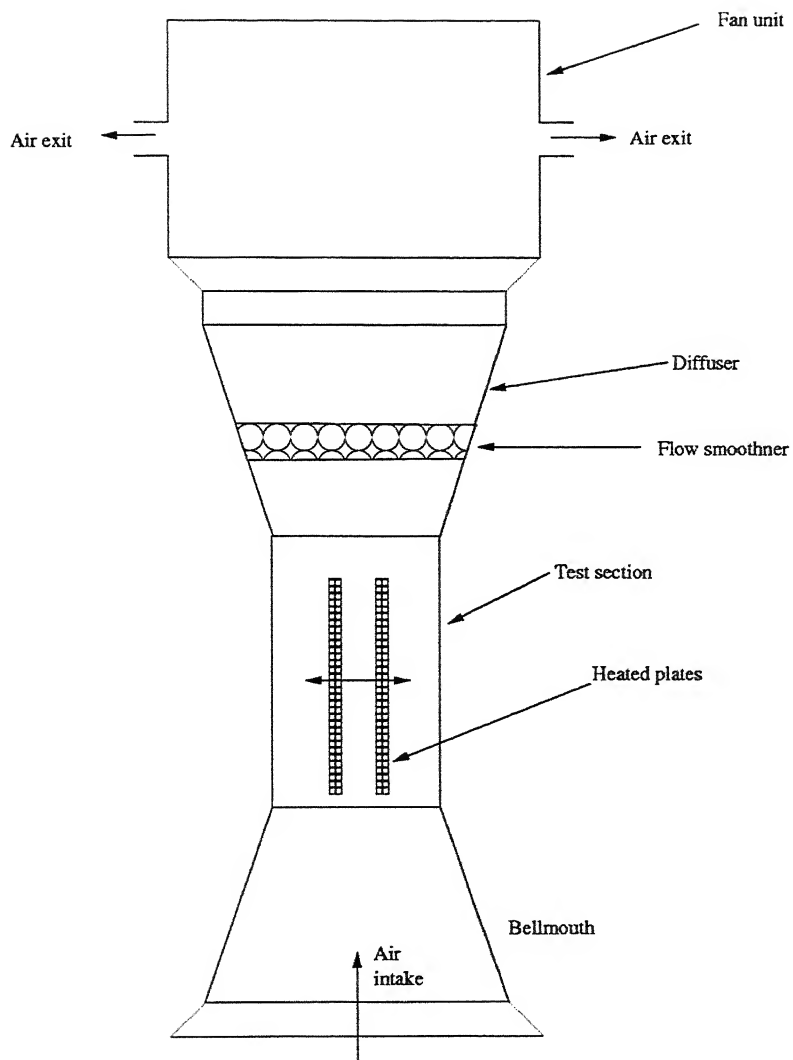


Figure 4.3 Schematic Diagram of the Experimental Test Rig

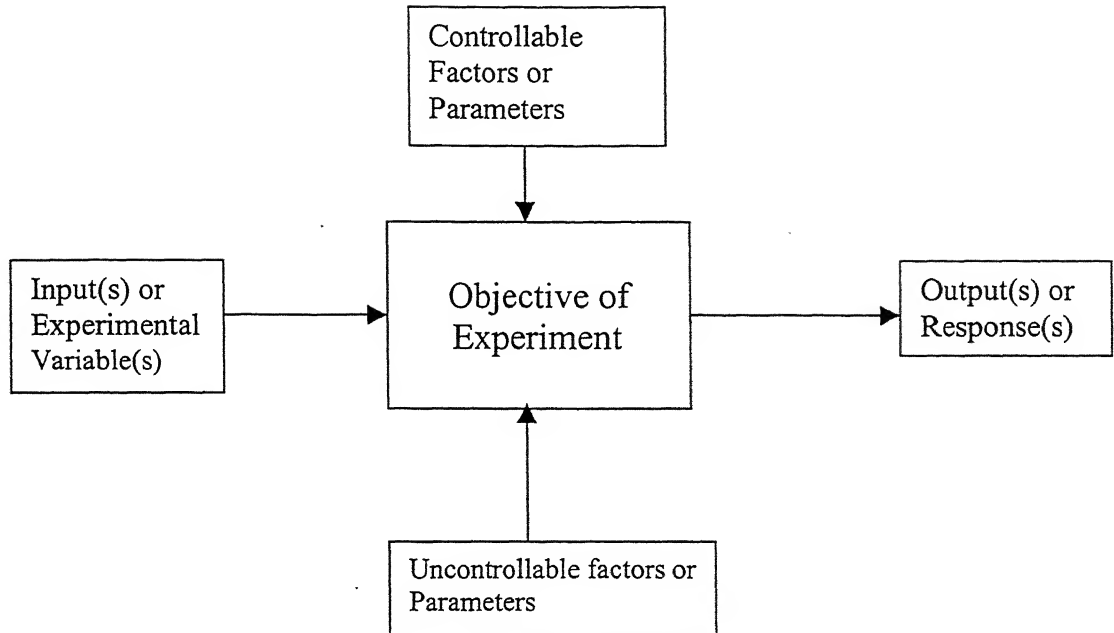


Figure 4.2b: Block Diagram Representation of Experimental Test Rig.

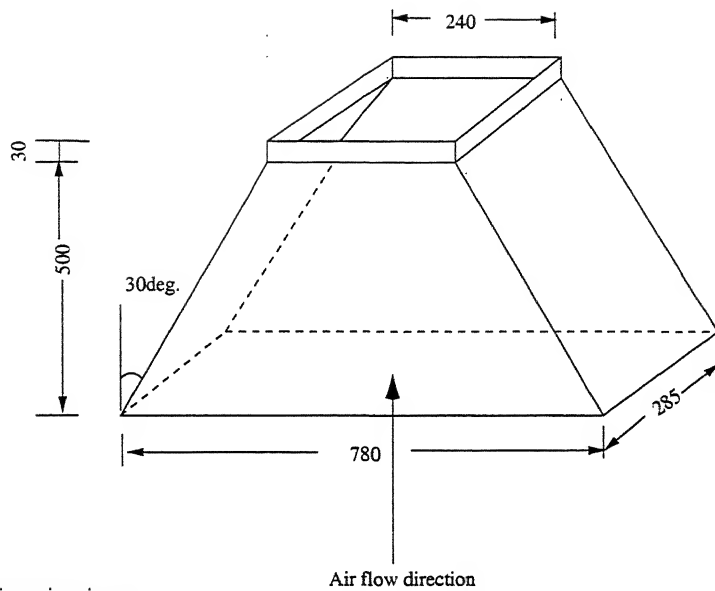
The whole test rig was 2.64m high, 0.84 m wide and 0.9m deep. The test rig consisted of the following components:

1. Air intake unit, 2. Test section, 3. Diffuser and
4. Suction chamber/ fan chamber or driving unit.

The full description of each component follows next.

4.2.2 Air Intake Unit

The dimensions of this component are shown in Fig. 4.4. The material used was galvanized iron (GI).



All dimensions in mm.

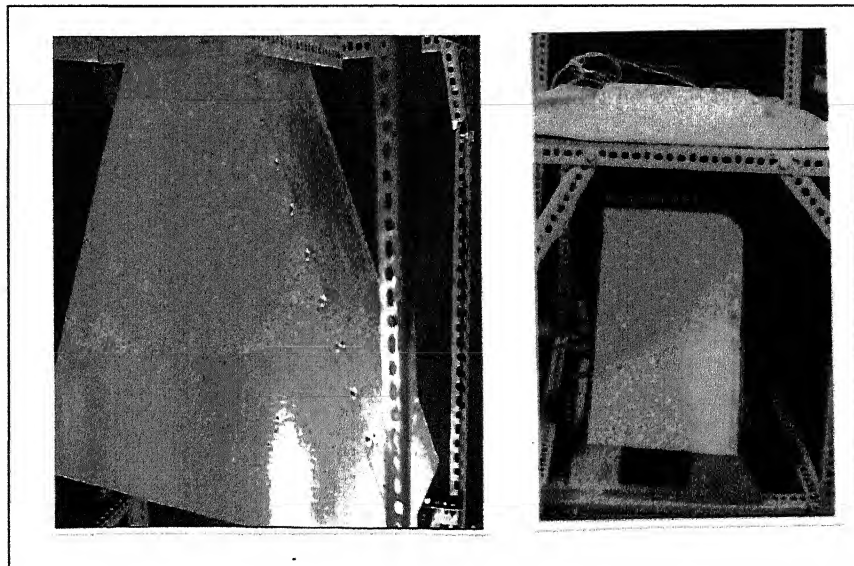


Figure 4.4 Inlet Section

.2.3 Test Section

The cross sectional area of the test section basically determined the overall size of the test rig. Since the size of the facility will be the primary factor in determining the structural costs, and the power cost, so test section was the main part of the test rig. The test section size, design and inside air velocity determined the required power. Over the years many shapes have been used for test sections, including round, elliptical, square, rectangular, hexagonal, octagonal, rectangular with filled corners, flat ceiling and floor with half round ends. The difference in losses in the test section due to cross sectional shape was negligible. Therefore, the shape of the test section was based on the utility and considerations of the model to be tested. The length of the test section was also another factor to be considered. Since it effected the total power consumption, it was not longer than necessary. A practical detail in the test section design is the installation of sufficient windows for viewing it. In the course of testing it had become necessary to be able to view all parts of model: top, bottom, side, and as much of the front as was reasonably practical. For safety reasons, windows in the test section were made of shatter resistant material. For many years the material of the choice was plate safety glass. The dimensions of the test section made in the present work are shown in the figure 4.5 Glasses of 15mm thickness were fixed using aluminum angles; which also acted as heat insulators and test section shrouding. Heated plates simulating the PCBs were placed inside this section.

4.2.3a Details of Heated Plates

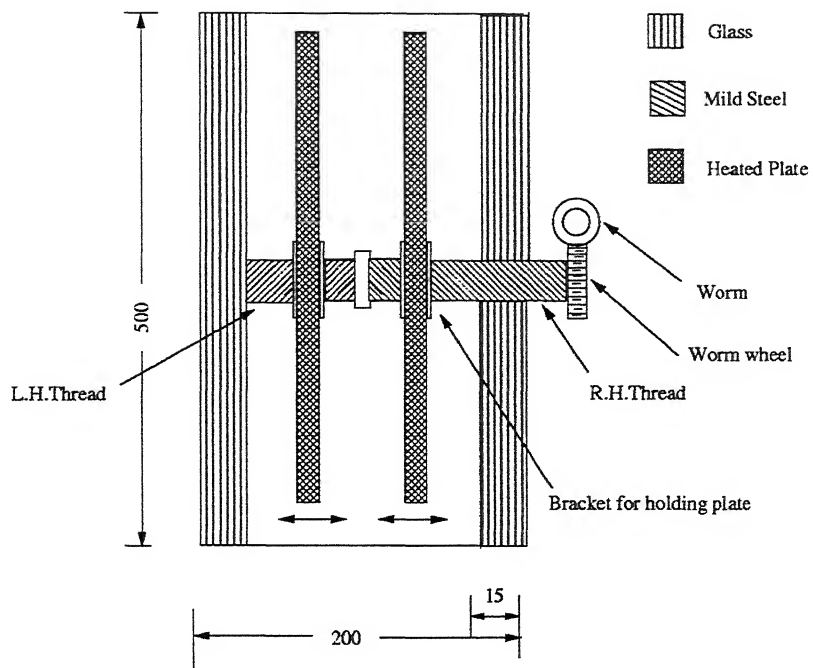
Figures 4.6a, b, c shows the inner view of a plate. Each divided part had a maximum heat dissipating capacity of 300W. Asbestos was placed beneath the heating elements to restrict the heat transfer from the back of the plate. For controlling the separation between plates a lead-screw arrangement was designed and fabricated (see Fig. 4.7). The arrangement enabled the plate movement in such a way that the channel between the two plates always lay at the center of the test section. This also helped in keeping the plates parallel to each other. Pulleys and belts along with driving motors were used for rotating the lead screws.

4.2.4 Diffuser

The detailed dimensions of this component are shown in Fig. 4.8. The material used in making the diffuser was perspex. Diffusers are sensitive to design errors that may cause either intermittent separation or steady separation. These separations can be hard to find and can cause vibration; oscillating fan loading, oscillation in test-section velocities (often called surging), and increased losses in the tunnel downstream of their origin.

4.2.4a Turbulence Reduction

Turbulence in the test section was reduced by the installation of honeycombs and screens. Different types of honeycombs were used. Fig.4.10 shows four of them. Placing honeycombs or screens in the tunnel increased the pressure drop, which lead to increased power for the same flow rate. The baffle plates were placed at a distance of 190mm from



All dimensions in mm.

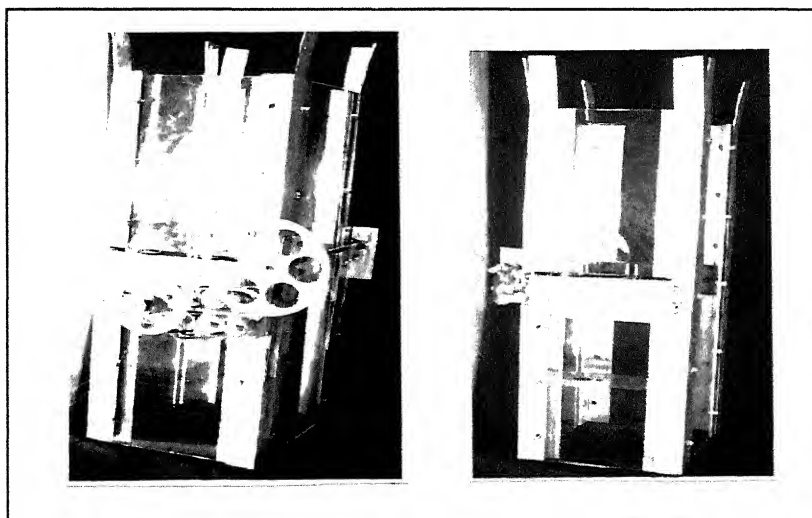


Figure 4.5 Test Section

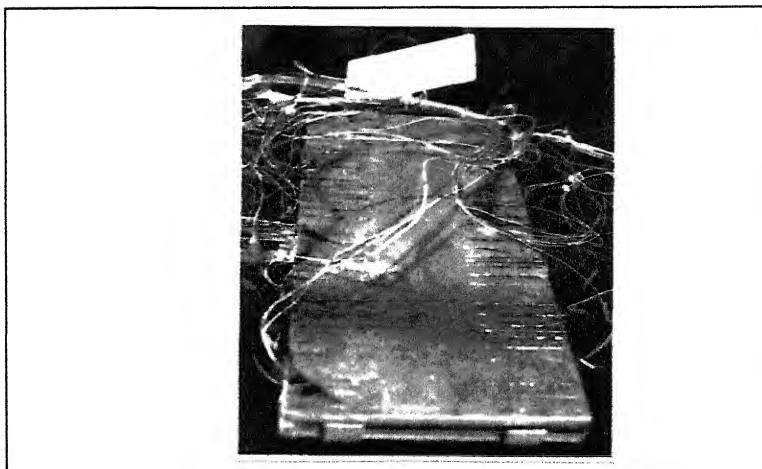
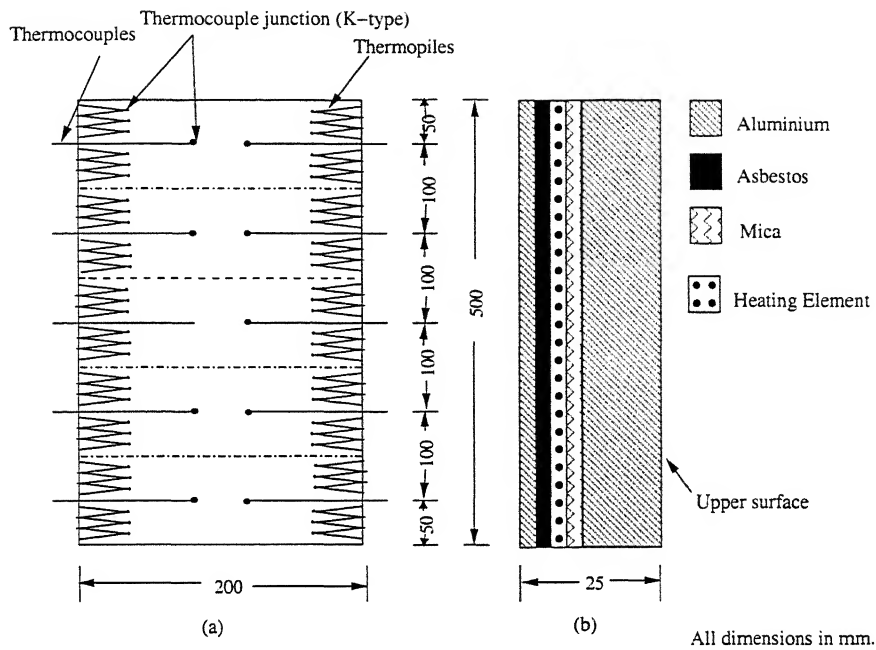
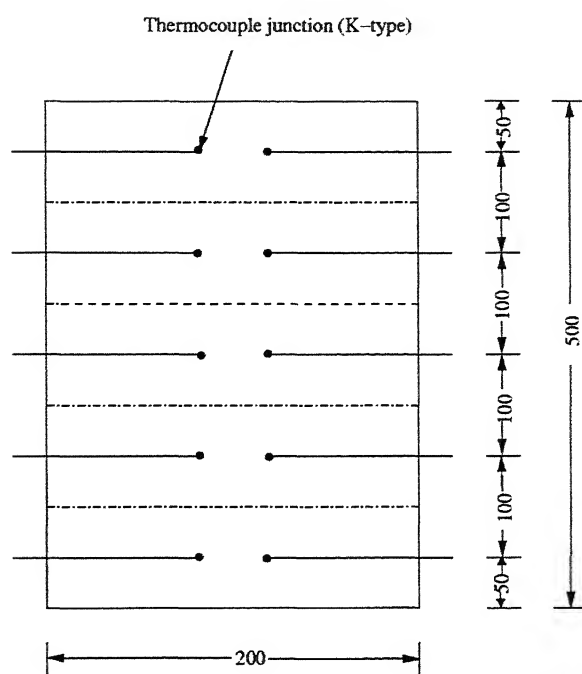


Figure 4.6(a) Thermocouple Arrangement on Front Surface of Heated Plate Surface (Plate 1)

Figure 4.6(b) Cross Sectional View of Heated Plate



All dimensions in mm.

Figure 4.6(c) Thermocouple Arrangement on Front Surface of Heated Plate (plate 2)

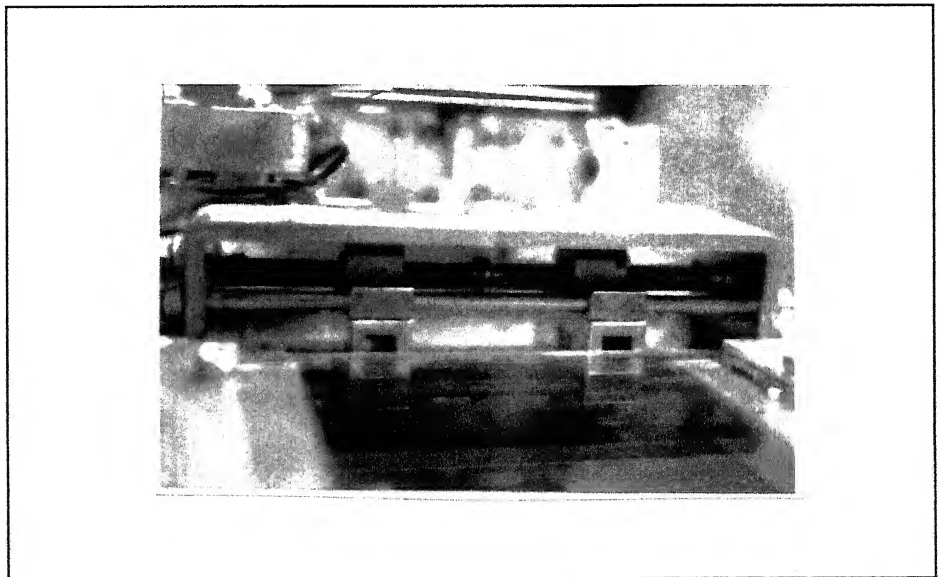
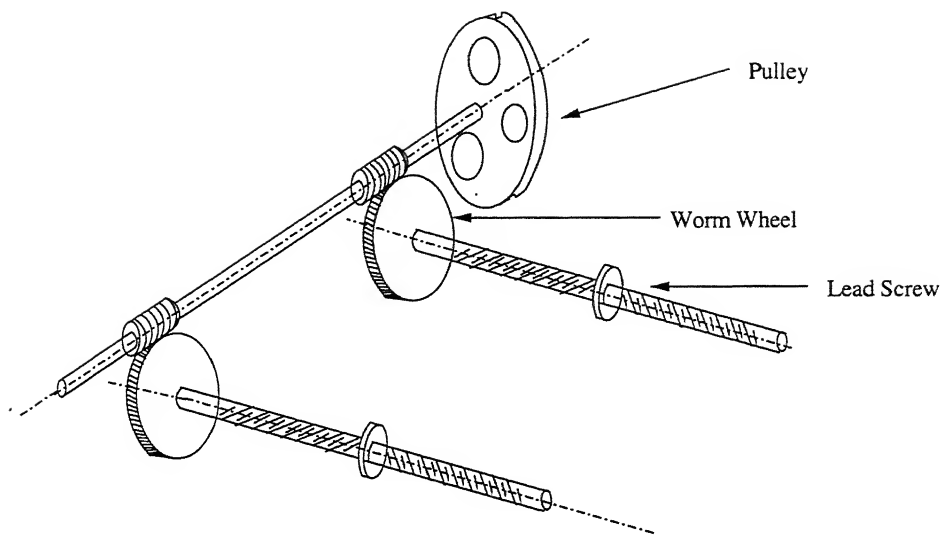
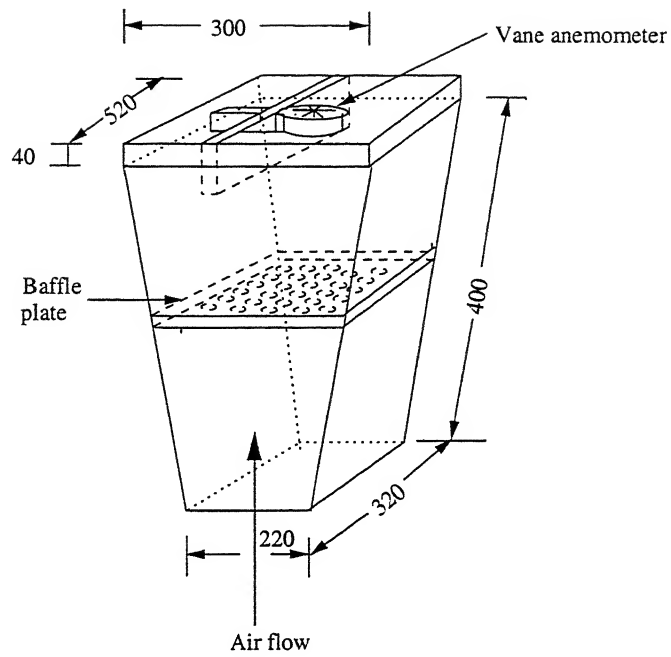


Figure 4.7 Lead Screw Arrangement



All dimensions in mm.

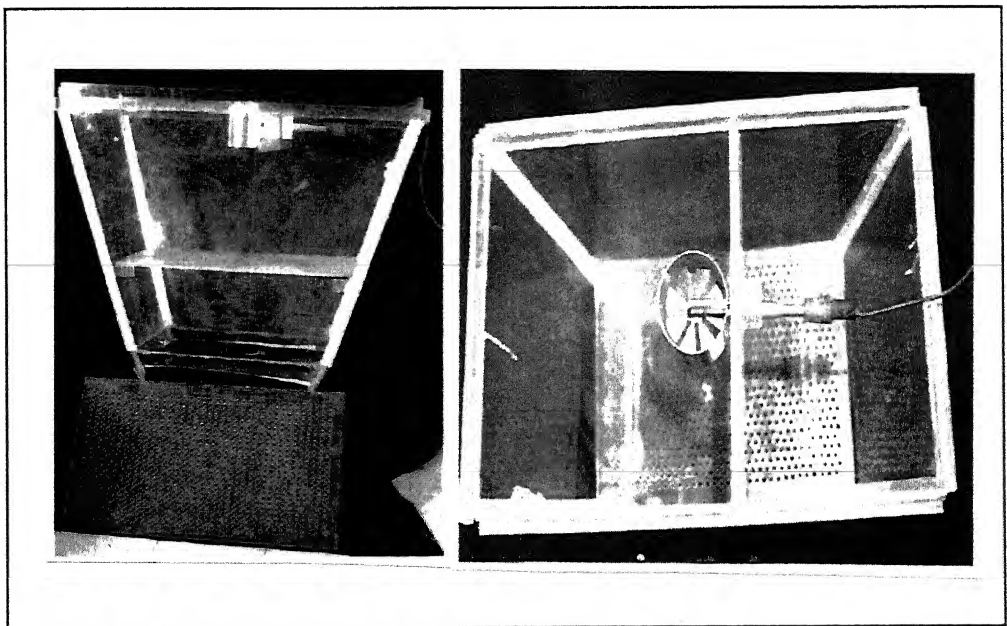
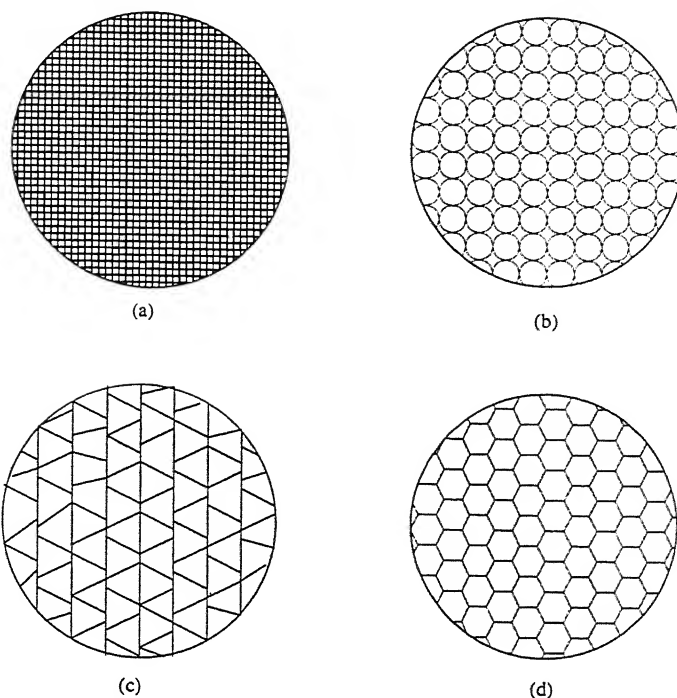


Figure 4.8 Diffuser

the bottom of this part. Vane anemometer was placed at its top to measure the air velocity at the center of the cross section.

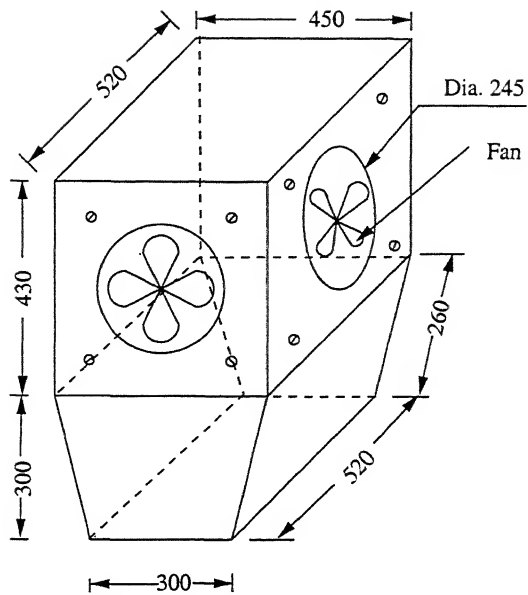


(a) Square web (b) Circular web (c) Triangular web (d) Hexagonal web

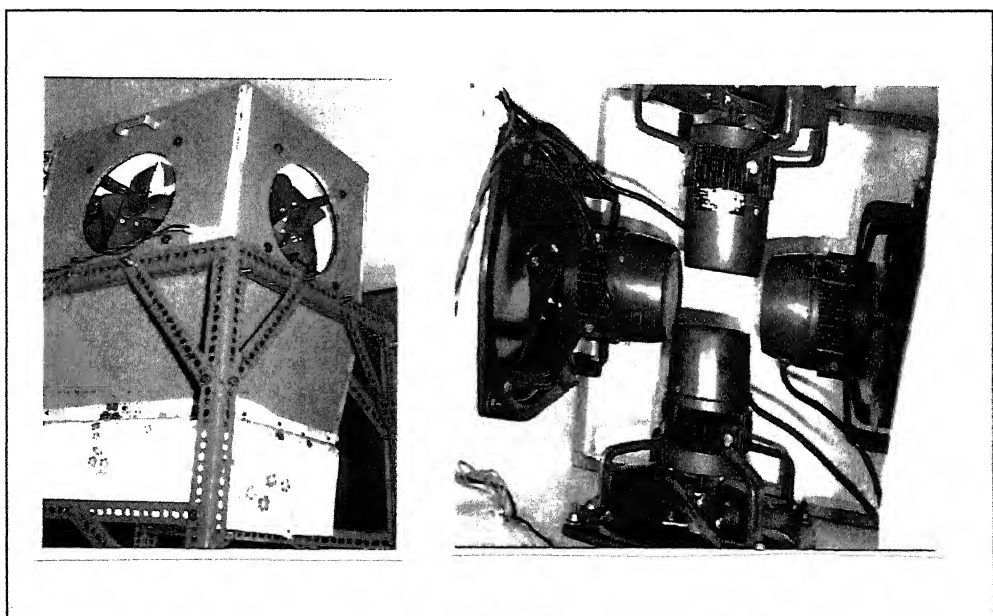
Figure 4.10 Four Types of Honeycomb

4.2.5 Suction Chamber

Since the thrust of the fan and the drag of the various tunnel component vary with the square of the fan r.p.m, it would appear that to maintain an even velocity front in the test section, speed adjustments were made by varying fan r.p.m. rather than pitch. Inside a wooden box having dimensions as shown in the Fig.4.9, four small exhaust fans (with a discharge rate of $0.2 \text{ m}^3/\text{s}$ at a rated speed of 1440 r.p.m.) were placed to create a pressure differential across the channel. Single fan of large discharge rate was not used to avoid inherent vibration problems. Arrangement was used to regulate the air discharge by controlling the power supplied to the fans.



All dimensions in mm.



4.3 Thermocouple Arrangement

4.3.1 At Inlet

Five thermocouples were placed at the entry to the test section to measure the air inlet temperatures as shown in the Fig. 4.11.

4.3.2 On the Plate

Figures 4.6a, b and c show the thermocouple arrangement on the heated plates. On one plate thermopiles were placed to measure the temperature difference across its faces (which will be used to calculate heat flux across the plate surface), while thermocouples were placed on the upper side of each plate to monitor and control the temperature on the plate surfaces.

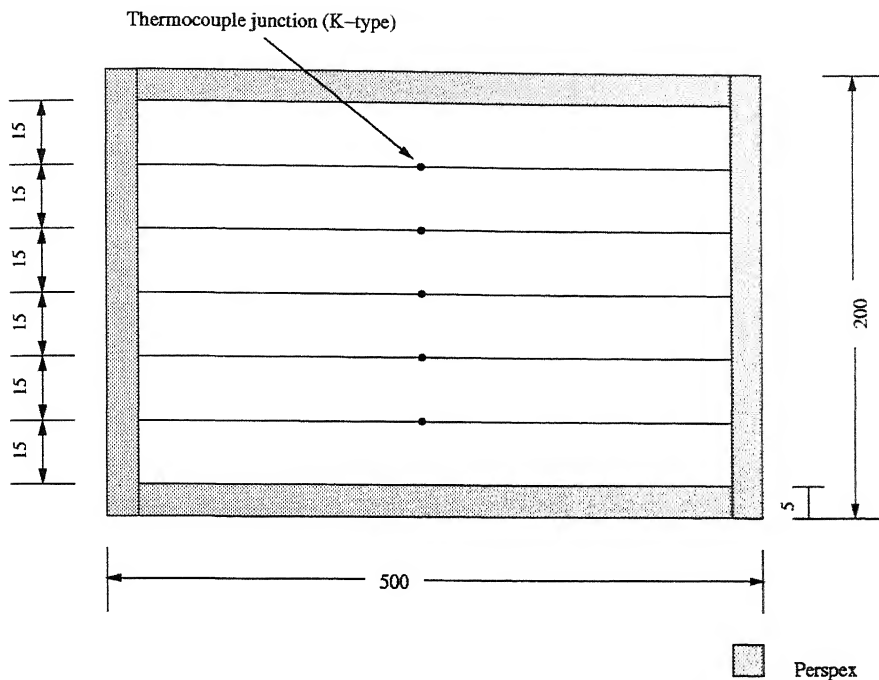
4.3.3 At Exit

Figure 4.12 shows the arrangement used to measure the temperature at the exit of the channel.

4.4 Experimental Uncertainties

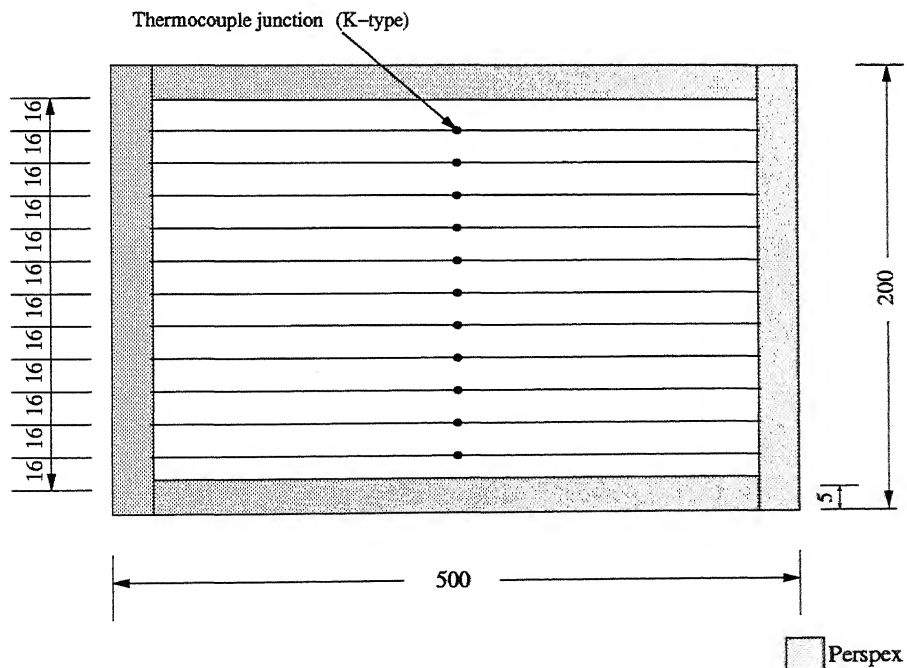
Errors in the experimental may arise due to various reasons. These can be classified as:

1. Systematic or determinate errors, arising as a result of poor calibration of instruments and,



All dimensions in mm.

Figure 4.11 Thermocouple Arrangement at Test Section Inlet.



All dimensions in mm.

Figure 4.12 Thermocouple Arrangement at Test Section Exit

2. Random or unavoidable errors, arising as a result of uncertainty with the accuracy of measuring instrument and the ability of the operator to read such instruments both accurately and consistently.

While no attempts were made in the present study to quantify these errors, all feasible efforts within the practical limits were implemented to ensure that the possible errors are minimized.

Chapter 5

RESULTS AND DISCUSSION

5.1 Introduction

Combined free and forced convection flows were studied extensively in the present work, yet a lot of questions still remain to be unanswered on this subject. The present work introduced an experimental method for analyzing mixed convection effects in Printed Circuit Boards (PCBs) by simulating them as vertical heated plates. The analysis presented here is for the condition of uniform heat flux. Since, for proper working of an electronic component its surface temperature should be lower than some specified temperature limit, so the experimental data were taken while limiting the temperature of the top part of the plate in the channel to the maximum specified temperature limit of 85°C (for this work). Study has been made for static pressure differences of 0 Pa, 4.4 Pa and 8.8 Pa and the plate spacing was allowed to vary in between 5mm and 75mm. Data were taken only after obtaining very stable thermal conditions or steady state observed in the apparatus (which took approximately 3-4 hours after the system had being energized). Air was taken as the working fluid. Subsequently, a large amount of data relating static pressure differences, plate spacing, air velocity, power input to the plates, exit air temperature and fan power input were recorded. The assumption of uniform air velocity over the whole cross

section is made and is best justified by the results of Dyer and Fowler [32]. Since, some of the heat generated inside the plate was, conducted from the plate to the clamping blocks and convected from the back face of the plate and therefore in order to calculate the heat transfer rate, a correction for these losses was made.

5.2 Heat Flux Distribution

Figure 5.1 shows the variation of plate heat flux, Q_f , with plate spacing, x , or different values of static pressures (0 Pa, 4.4 Pa and 8.8 Pa). It can be seen from the plot that as the plate spacing increases, the heat flux from the plate also increases, till it reaches a maximum value (for a fixed value of ΔP). Beyond this the value of heat flux decreases or increases insignificantly.

5.3 Total Heat Transfer Distribution

Figure 5.2 shows variation of total heat transfer, Q_t , with plate spacing, x , for different values of ΔP . For natural convection ($\Delta P=0$ Pa) the maximum heat transfer value occurred at $x=22.5$ mm and for $\Delta P= 4.4$ Pa and 8.8 Pa the corresponding values of x are 46mm and 47mm. These plate spacings can be taken as optimum plate spacings, x_{opt} . Typical value of maximum heat flux in case of pure natural convection is about 0.3 W/cm^2 at the optimum plate spacing of 22mm, which is in good agreement with the order of heat transfer handled by natural convection cooling. Figure 5.3 shows the variation of fan power consumption with plate heat flux. It is evident from the figure that to remove the more heat flux from the plate, more fan power is needed.

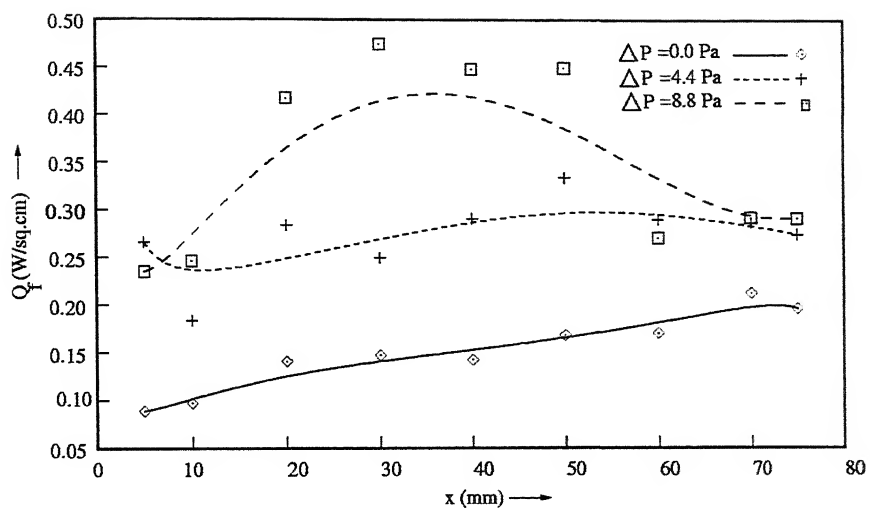


Figure 5.1 Variation of Plate Heat flux with Plate Spacing for Different Static Pressures

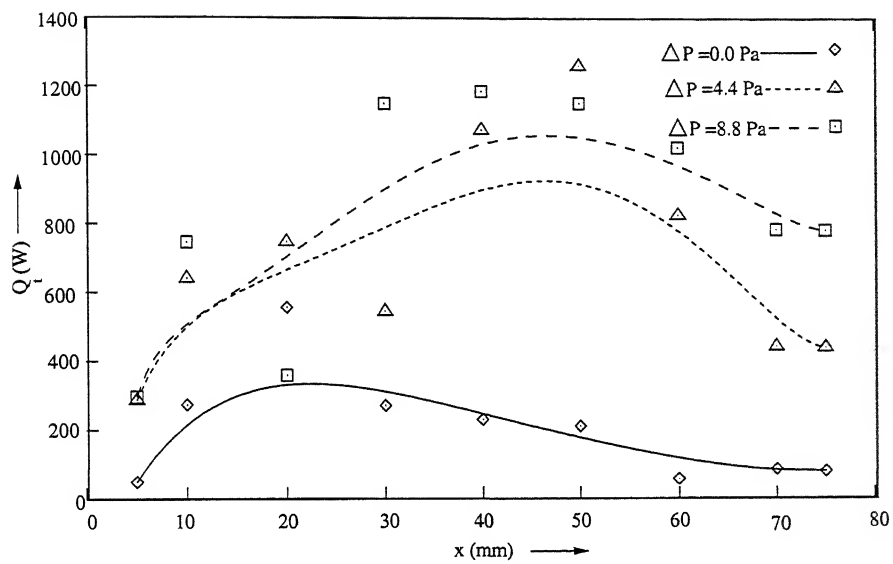


Figure 5.2 Variation of Total Heat Transfer with Plate Spacing for Different Static Pressures

5.4 Driving Power Distribution

The overall power requirement for running any electronic equipment or device is the sum total of the power consumed by its electronic circuitry and the power needed for driving the cooling unit. Ratio between these two power requirements must be within an acceptable economical limit. Figure 5.4 shows the variation of fan power or driving power with plate spacing for $\Delta P=0$ Pa, 4.4 Pa and 8.8 Pa. It is evident from the figure that as the plate spacing increases the more fan power is required to create the same pressure difference across the channel for a fixed value of ΔP . One can also look back at figure 5.2 and observe that in order to achieve higher cooling rates at any given spacing, more static pressure will be needed, which means further increase in driving power requirements and hence, increased cost of cooling. The nature of the curve is like a straight line. Or in other words, for the same fan power input, the smaller plate spacing results in greater pressure differential than larger plate spacing.

5.5 Exit Temperature Distribution for Air

Variation of air exit temperature along the channel width ($b^*=b/B$) for different values of static pressures and for a given value of plate spacing is shown in each of the figures 5.5. The temperature profile is of parabolic nature until $x=30$ mm and after that two individual peaks appear (which is due to the two separate boundary layers in the channel). It may be noted from the plots that for a fixed plate spacing the exit temperature is greater for larger ΔP compared to that for its smaller value. The trough in between these two peaks is steeper in the case of natural convection than in mixed convection. This is due to the better mixing of air in the case of mixed convection.

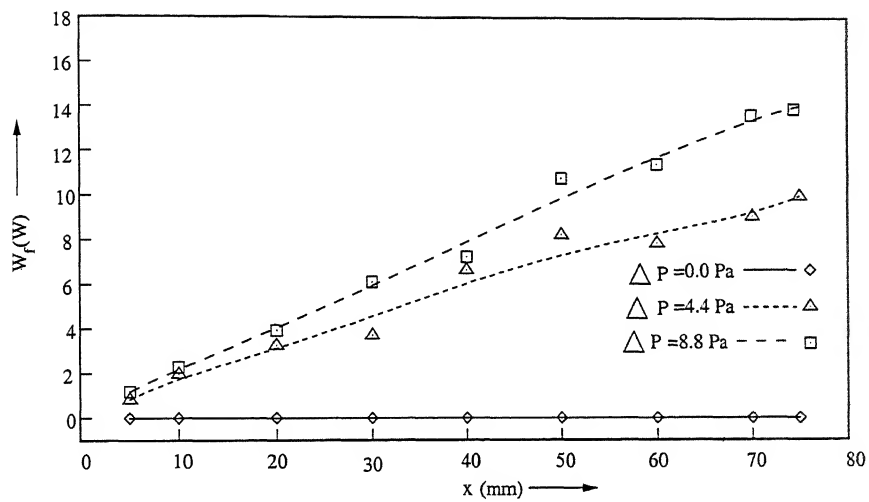
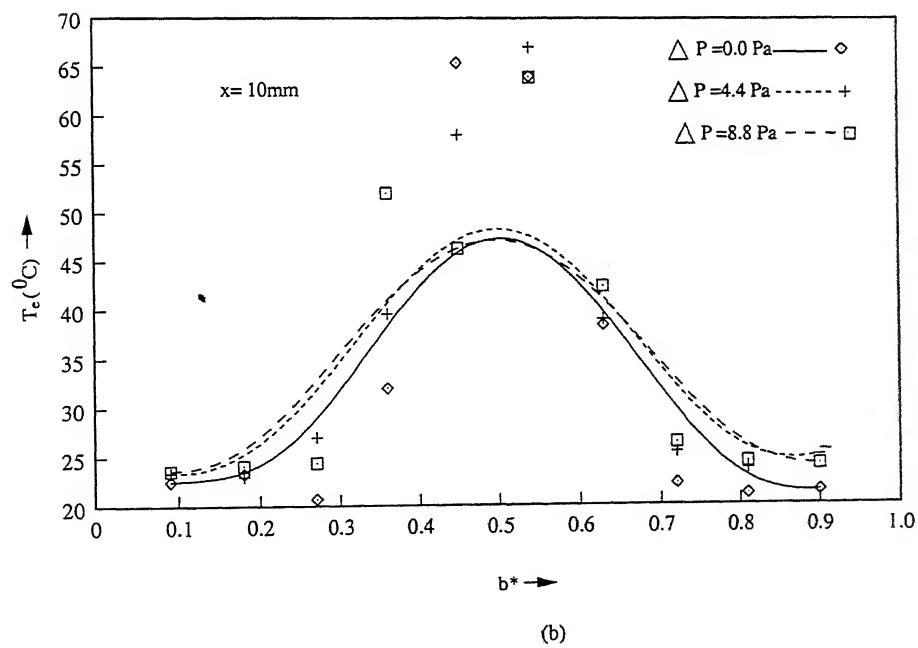
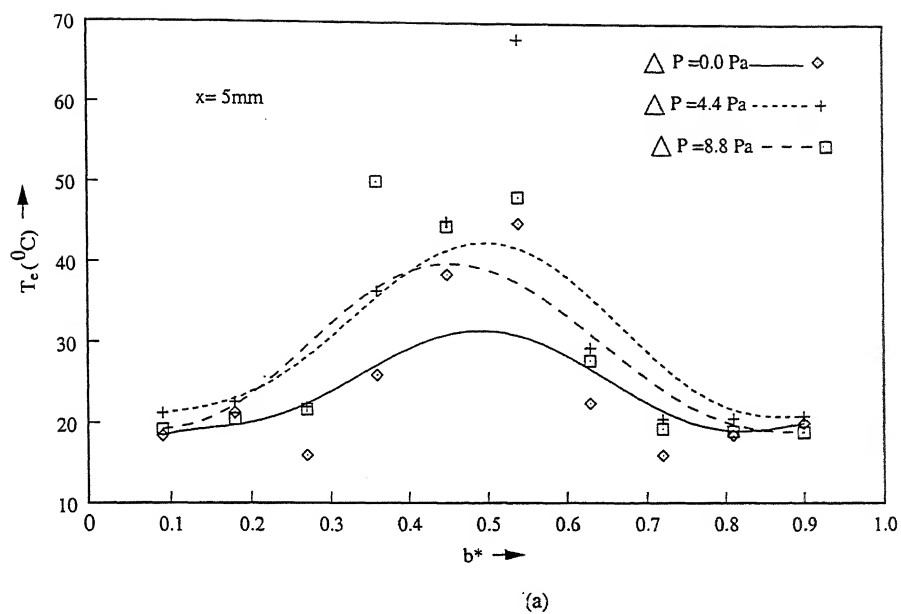
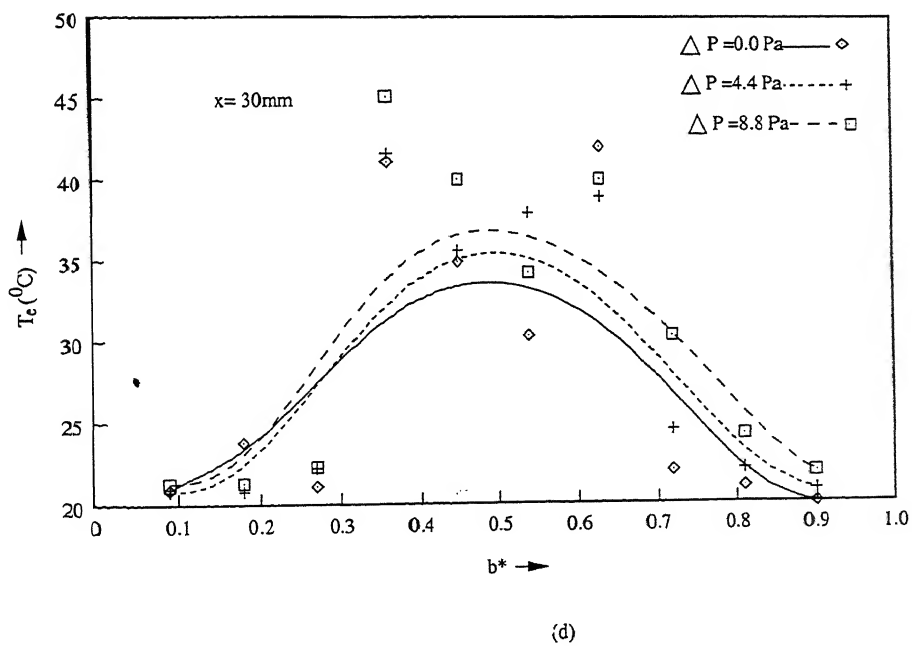
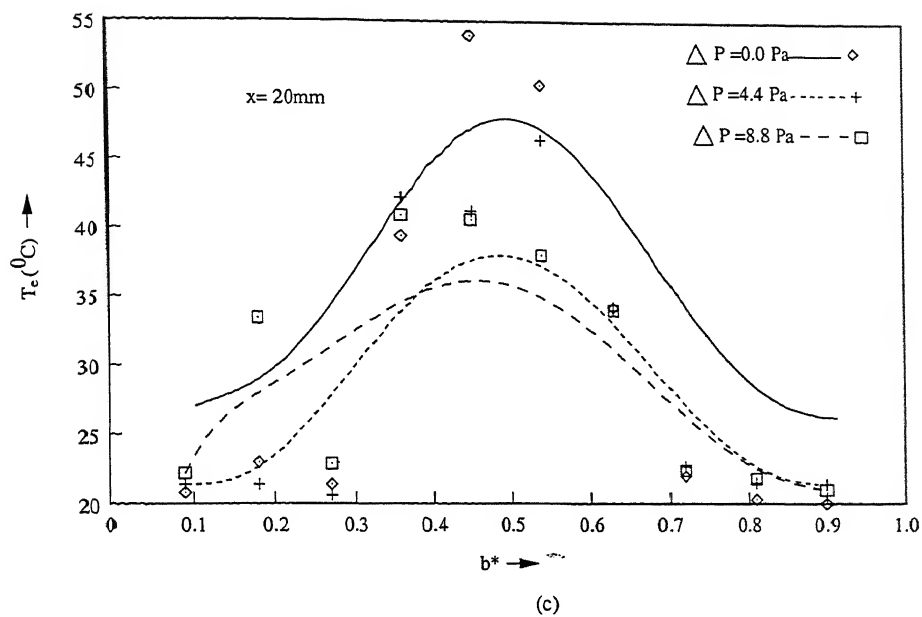
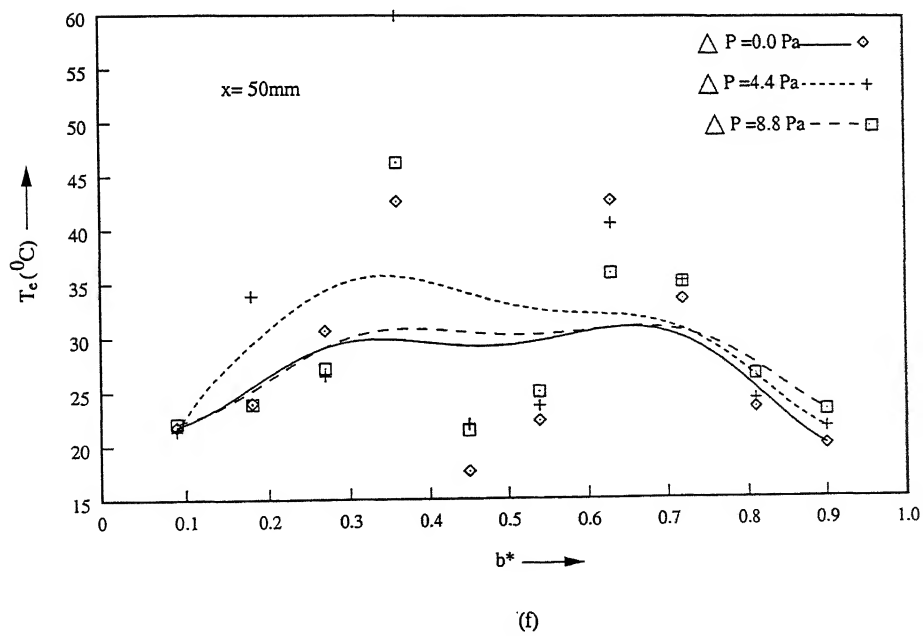
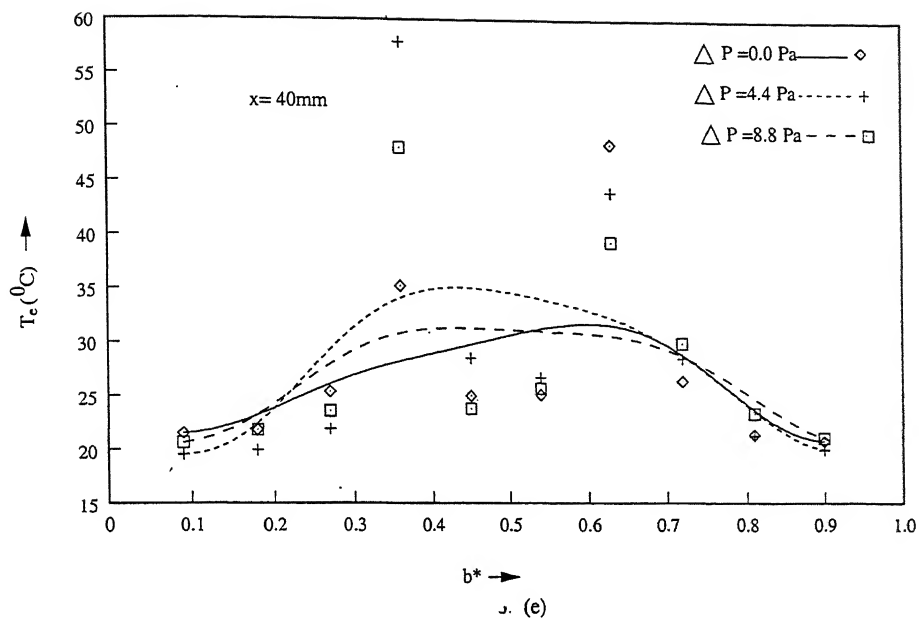
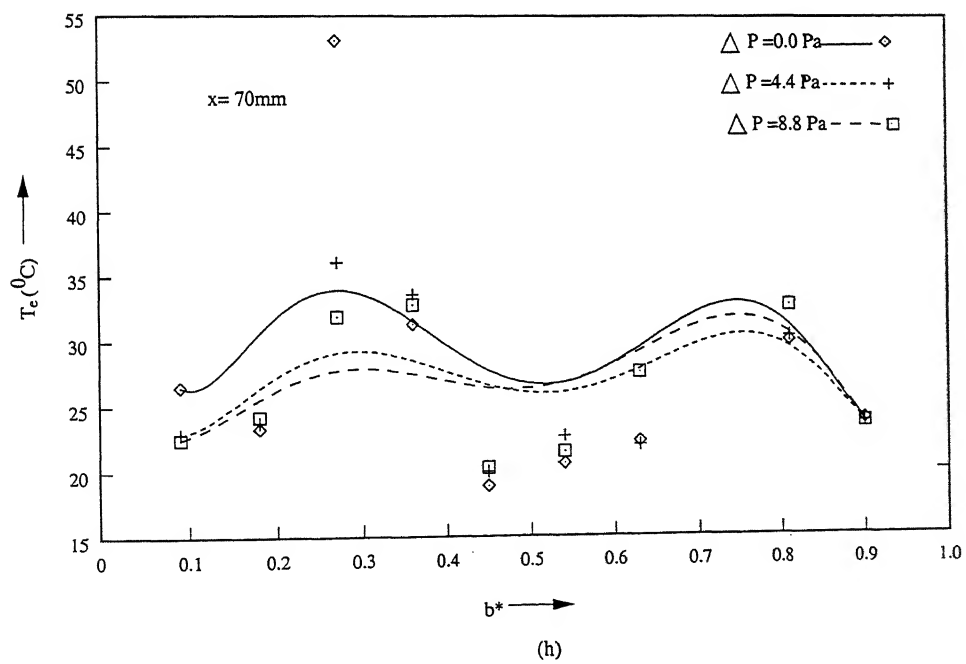
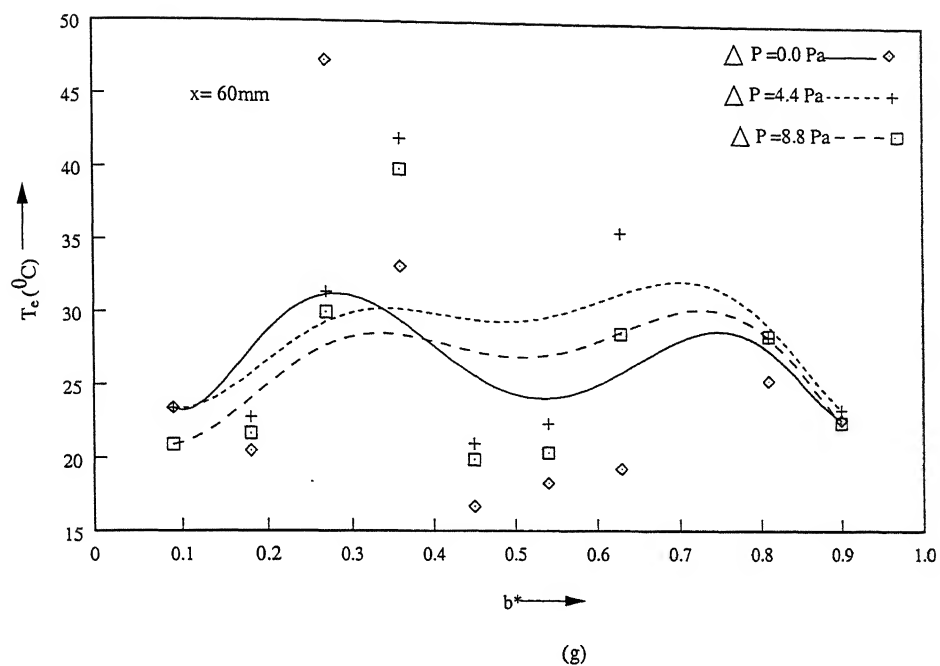


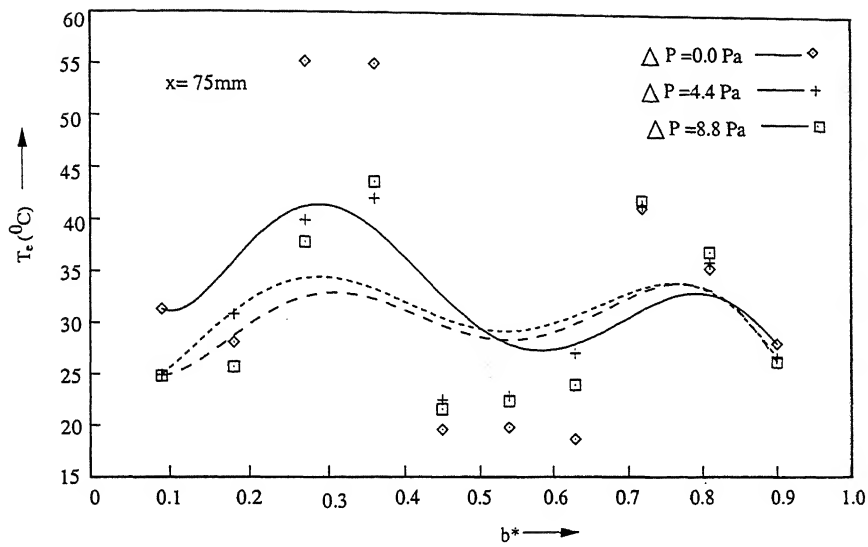
Figure 5.4 Variation of Fan Power With Plate Spacing for Different Static Pressures











(i)

Figure 5.5 Variation of Air Exit Temperature with Thermocouple Location for Different Static Pressures and Plate Spacings.

5.6 Optimum Heat Flux Distribution

The compactness of an electronic system always remains a prime factor governing its design. Even after adoption of large and very large circuit integration technologies, problems of proper configuration of the PCBs inside a well-shaped cabinet requires much consideration. If the PCBs are to be placed vertically oriented, they must be put inside the cabinet as close as possible. Now, it is the optimum spacing that governs the separation between two PCBs. The experimentally gathered data can be used for selecting an optimum spacing at given static pressure and some average heat flux value in the PCB. Figure 5.6 shows the variation of optimum heat flux (corresponding to optimum plate spacing) with optimum plate spacing. From the figure it can be seen that the optimum heat flux increases with an increase in the value of optimum plate spacing. Figure 5.7 shows the variation of optimum plate spacing with ΔP . It can be seen from the plot that as ΔP increases the value of plate spacing at which we get maximum heat transfer i.e. x_{opt} also increases, but after a value of $\Delta P \sim 8$ Pa the rise is not too significant, which clearly mean that for a limiting value of ΔP and corresponding to its optimum plate spacing x_{opt} we can not increase the heat transfer rate by simply increasing the ΔP further. At this point it is advisable to adopt some other techniques other than mixed convection to enhance the heat removal rate. Figure 5.8 shows the variation of optimum heat flux with static pressure differences. It may be concluded that it is not possible to increase the heat flux removal just by increasing the pressure differential across the channel. And after a limiting value of ΔP the power effectiveness (heat removal rate/fan power input) decreases, and also poses a serious limitation on the extent upto which the compactness can be achieved.

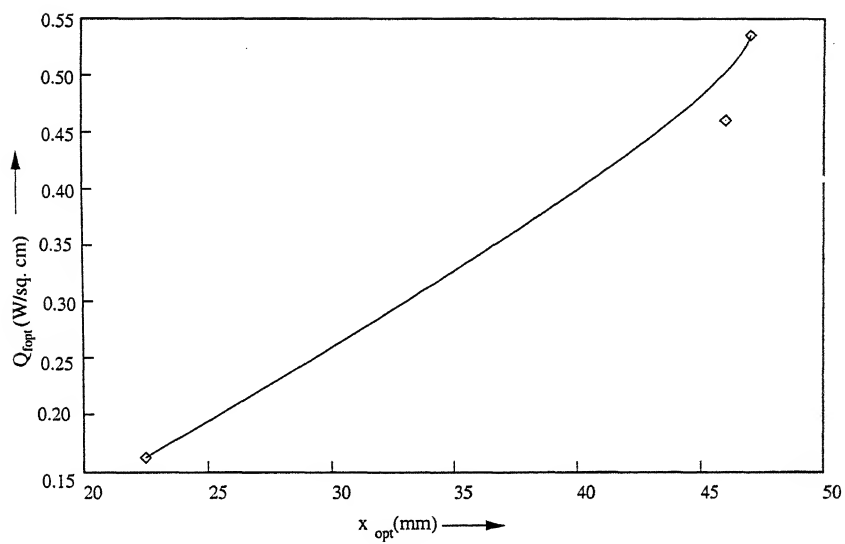


Figure 5.6 Variation of Heat Flux with Optimum Plate Spacing

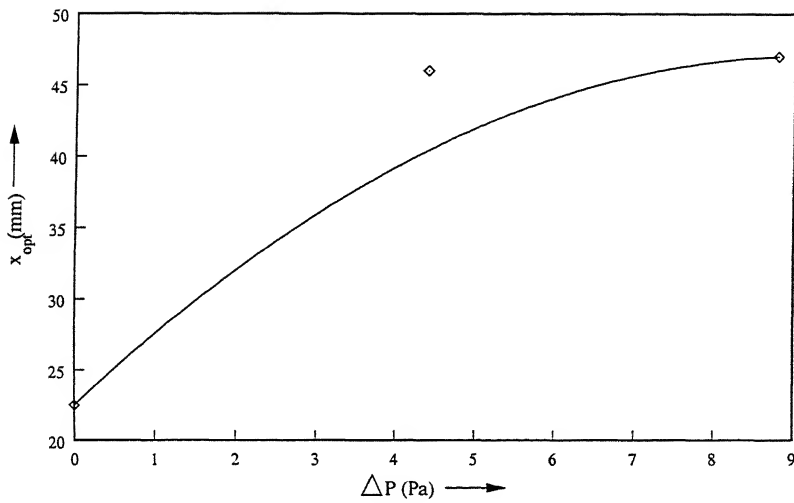


Figure 5.7 Variation of Optimal Plate Spacing with Static Pressure

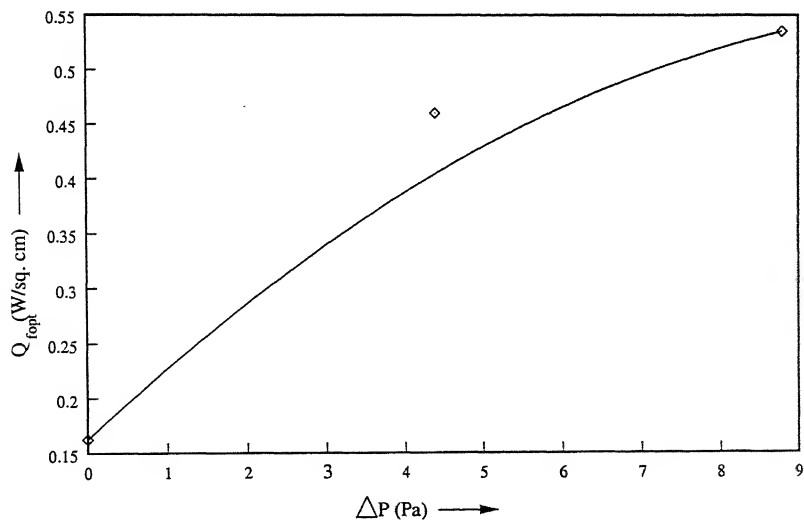


Figure 5.8 Variation of Optimal Heat Flux with Static Pressure

Figure 5.9 shows the three-dimensional variation of Grashoff number, Gr_y , (Grashoff number based on the distance from the channel entrance) with dimensionless space co-ordinates $y^*(=y/H)$ and $x^*(=x/X)$ for $\Delta P=0$ Pa, 4.4 Pa and 8.8 Pa. This plot compares the values of Grashoff number for natural and mixed convection heat transfer. The values of Grashoff number are smaller in the case of natural convection than in mixed convection. Figure 5.10,5.11,5.12 show these three plots separately. It may be concluded from the plots that as the plate spacing increases at fixed height on the plate the Grashoff number increases (for a fixed value of ΔP). It may also be seen that Grashoff number increases from bottom to the top of the plate for a fixed plate spacing and driving pressure.

5.8 Nusselt Number Variation

Figure 5.13 shows the three-dimensional variation of Nu_y (Nusselt number based on distance from the entrance) with dimensionless space co-ordinates y^* ($=y/H$) and x^* ($=x/X$). This plot shows a comparative trend in Nusselt numbers as ΔP increases. It can be observed from the figures 5.14,5.15,5.16 that as ΔP increases the values of Nusselt number increases for a fixed value of x^* and y^* . It could also be noticed that the values of Nusselt number increases as plate height increases. Figure 5.17 shows the three-dimensional surface indicating variation of Nu_y with x^* and ΔP . It could be seen from the plot that for lower values of ΔP the Nusselt number is low and the range of Nusselt number variations vertically along the plate surface is narrow too. As ΔP increases, the values of Nusselt number and its range increase.

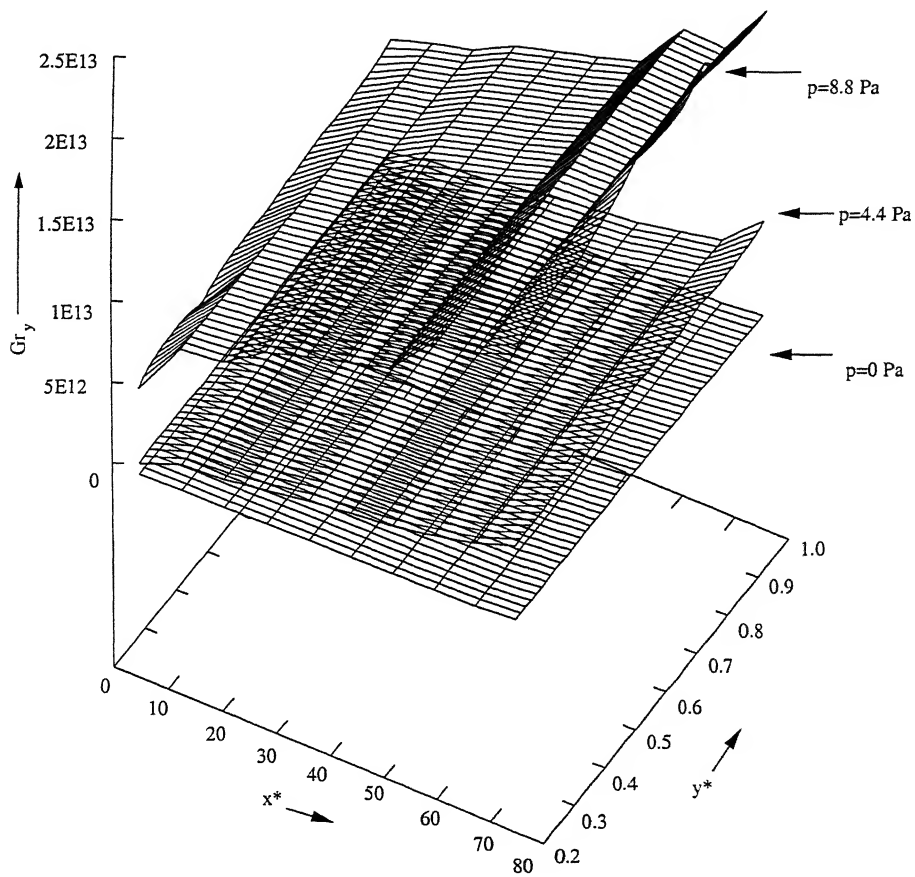


Figure 5.9 Three Dimensional Variation of Gr with Space co-ordinates for Different Static Pressures.

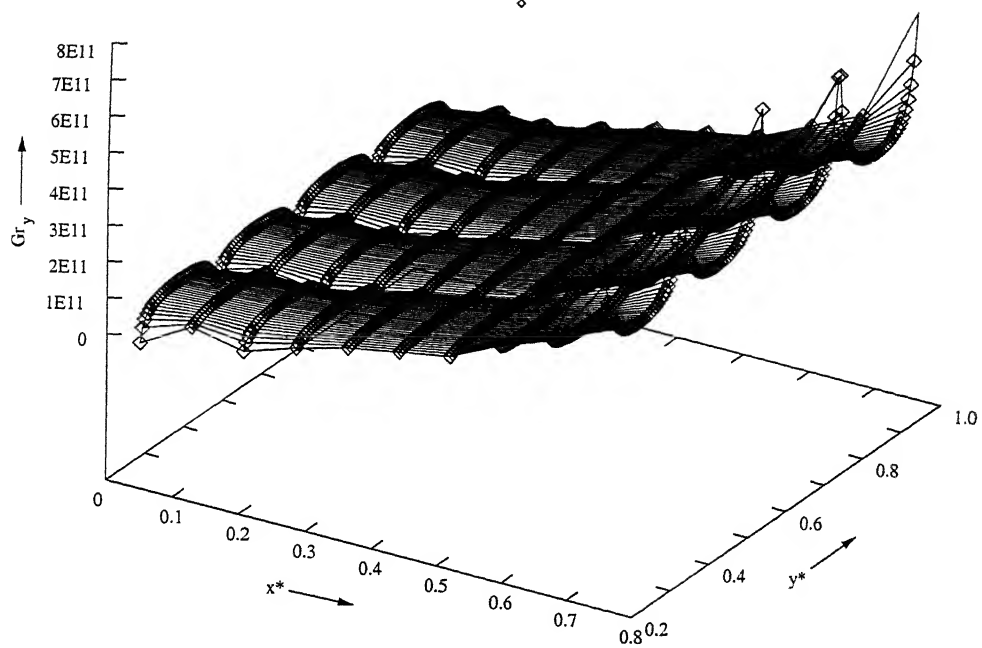


Figure 5.10 Three Dimensional Variation of Gr with Space co-ordinates for $\Delta P = 0.0Pa$

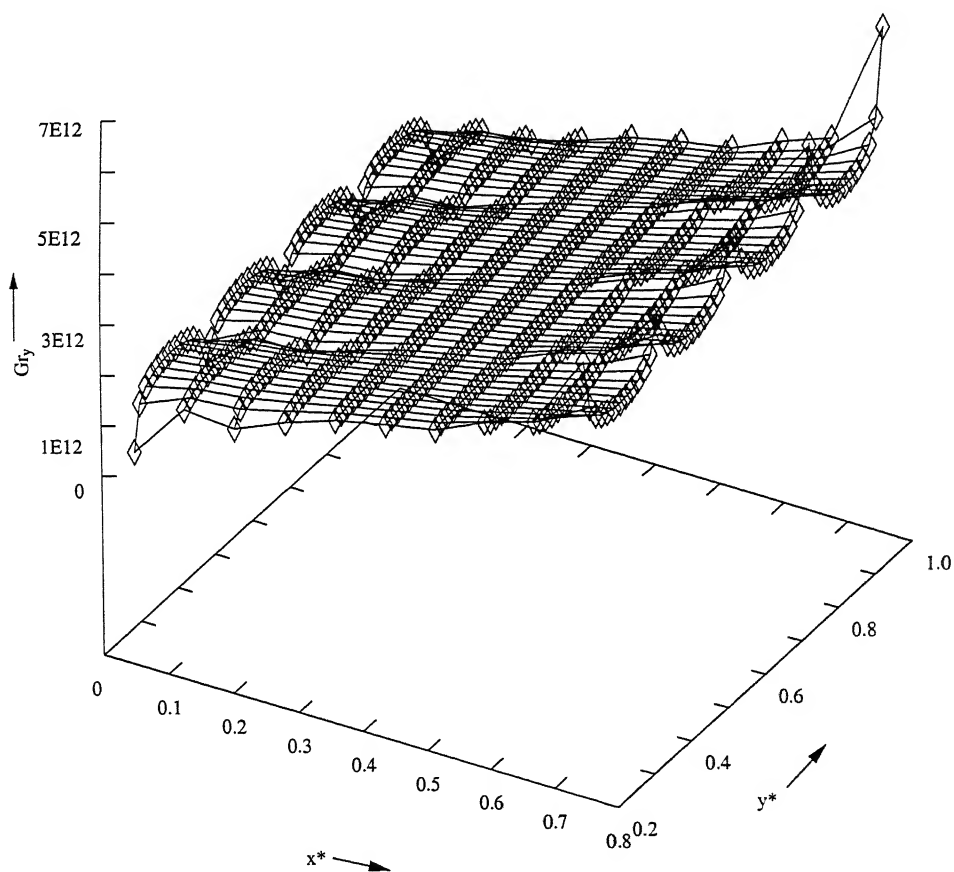


Figure 5.11 Three Dimensional Variation of Gr with Space co-ordinates
for $\Delta P = 4.4$ Pa

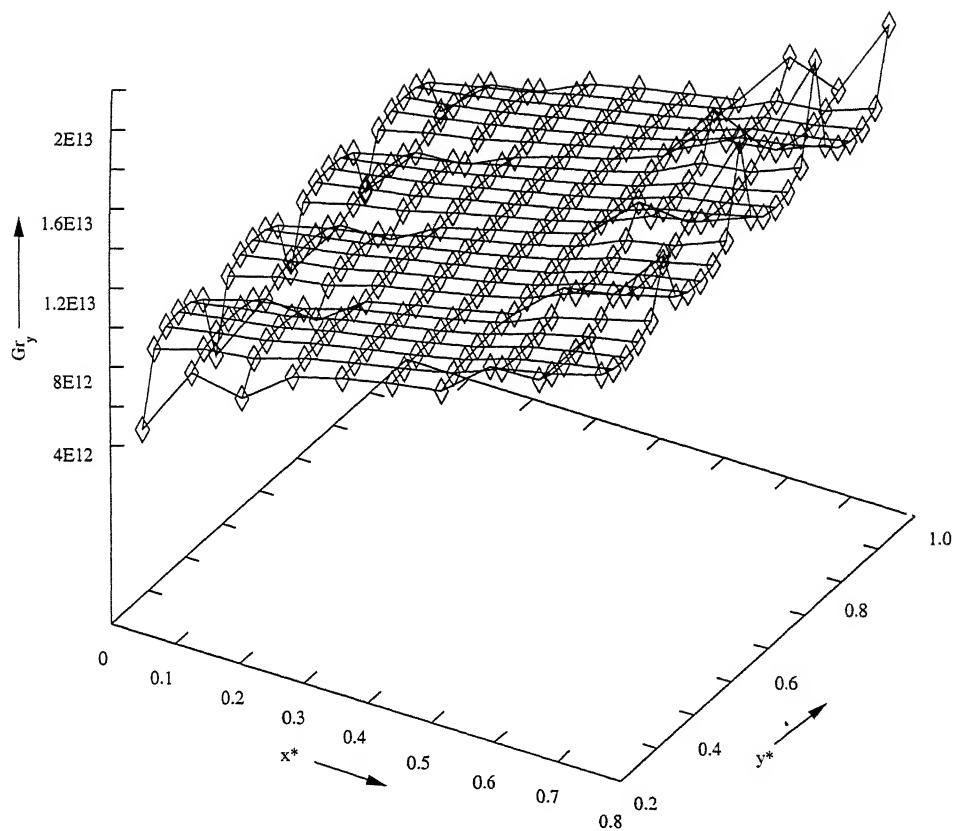


Figure 5.12 Three Dimensional Variation of Gr with Space co-ordinates for $\Delta P = 8.8$ Pa

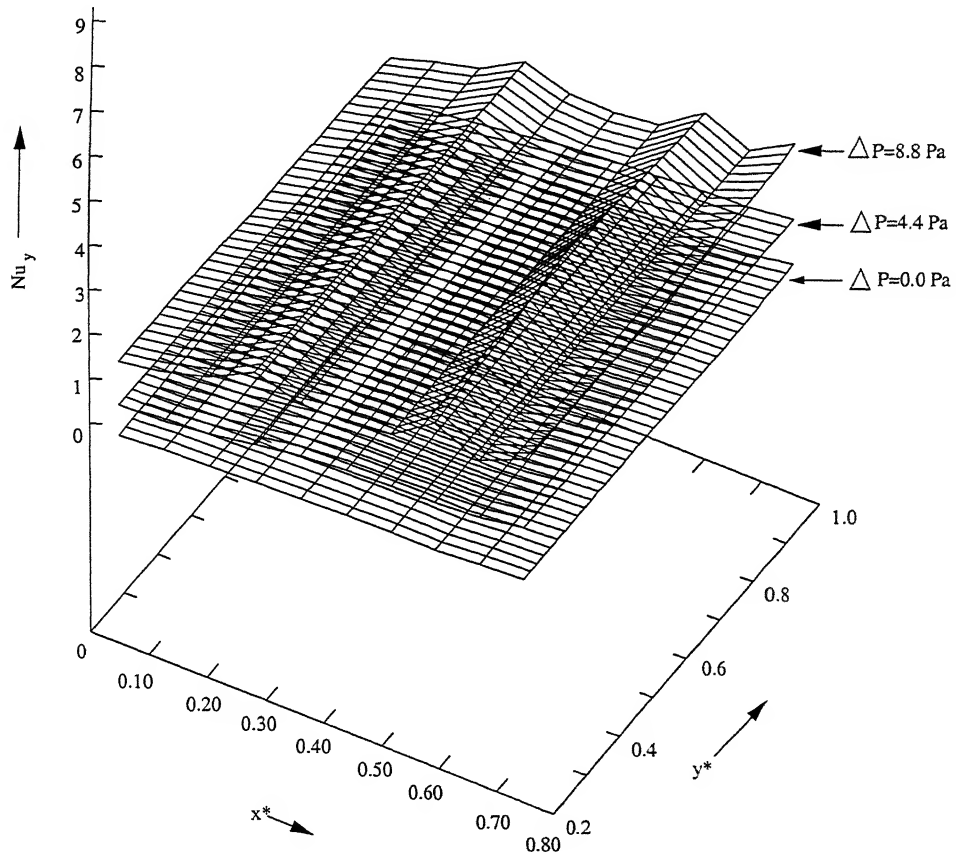


Figure 5.13 Three Dimensional Variation of Nu with Space co-ordinates and Static Pressures.

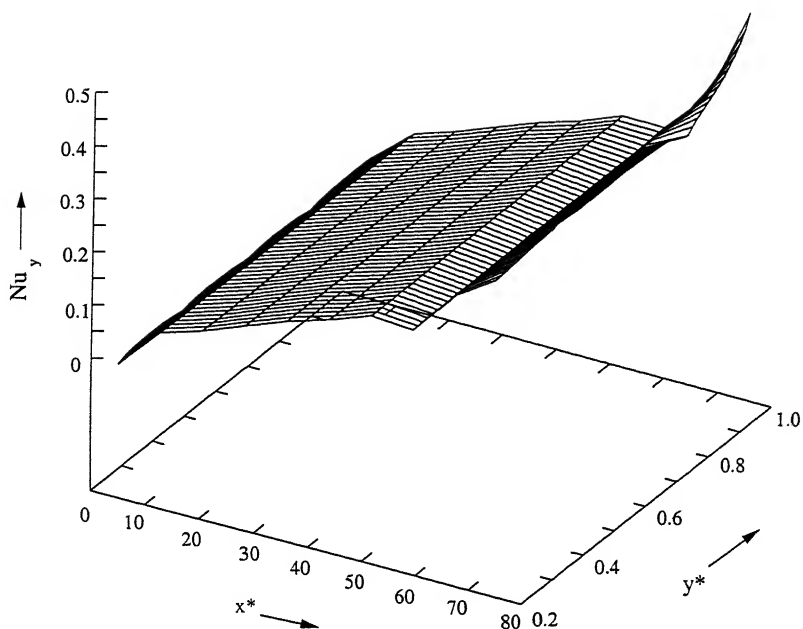


Figure 5.14 Three Dimensional Variation of Nu with Space co-ordinates for $\Delta P = 0.0$ Pa

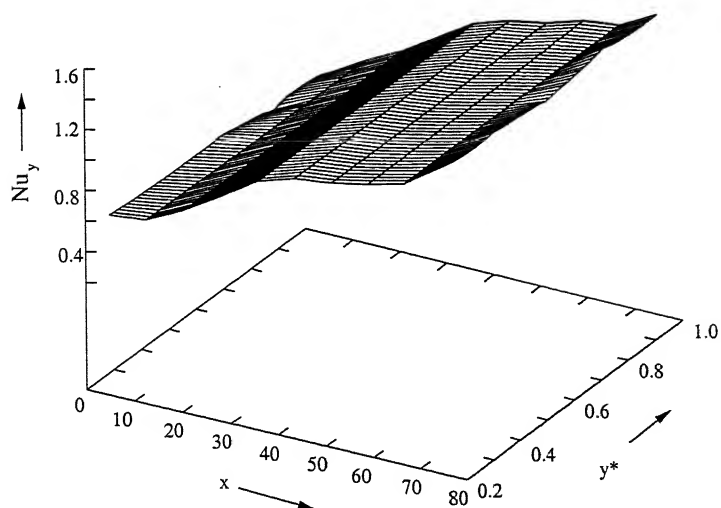
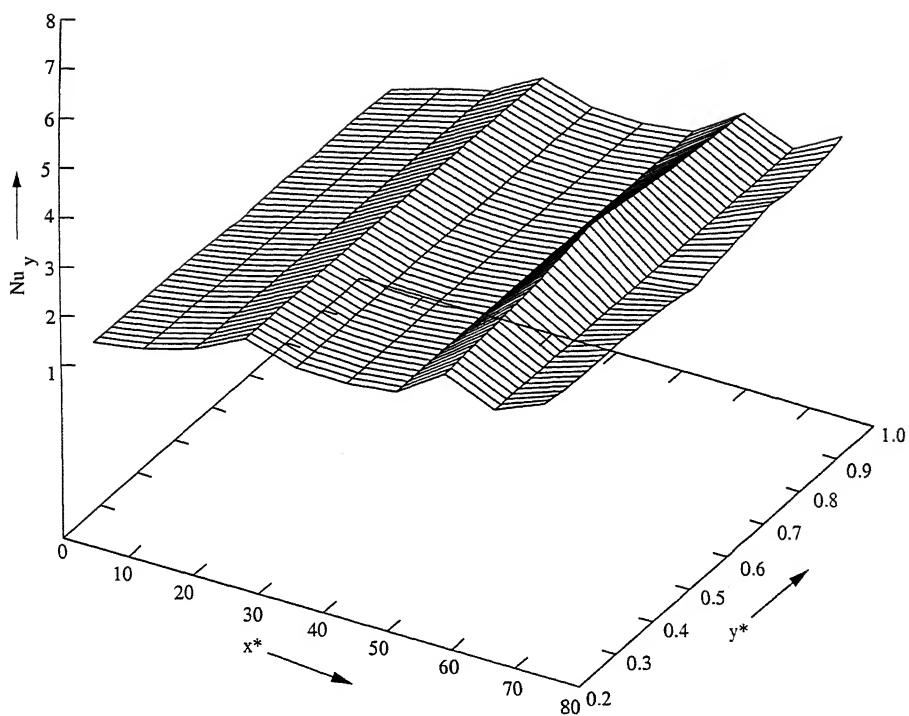


Figure 5.15 Three dimensional variation of Nu with space co-ordinates for $\Delta P = 4.4$ Pa



**Figure 5.16 Three Dimensional Variation of Nu with Space co-ordinates
for $\Delta P = 8.8$ Pa**

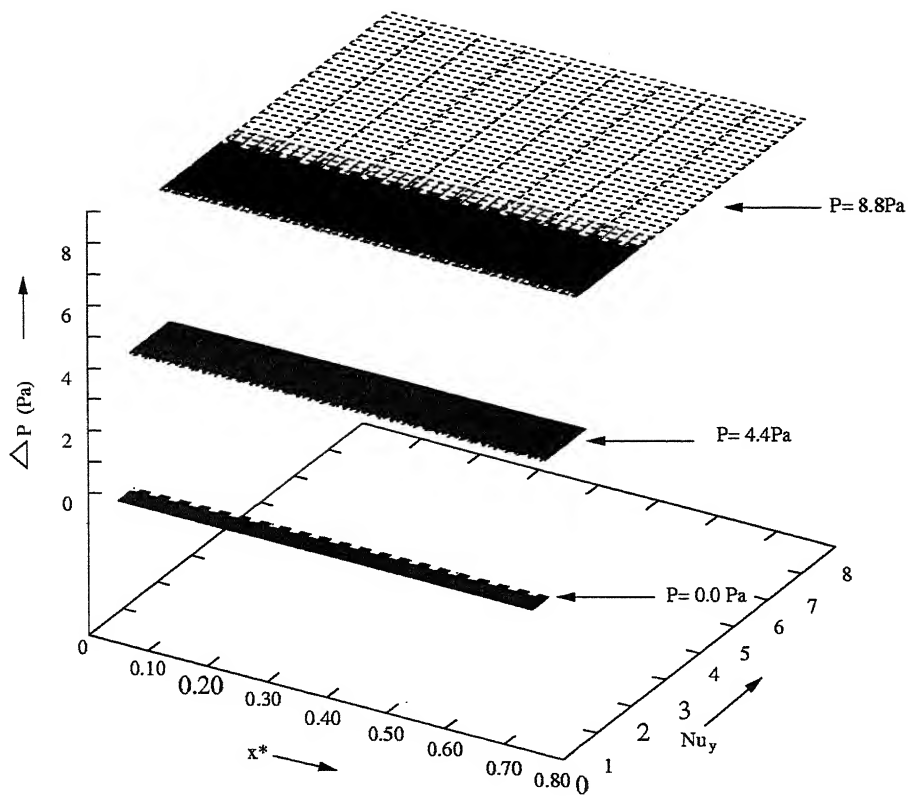


Figure 5.17 Three Dimensional Variation of Nu with Space co-ordinates and Static Pressure.

5.9 Conclusions

As outlined in the scope of the present study, an experimental test rig was designed and developed for conducting the experiments. Data relating total heat transfer rate and heat flux from the plate surfaces with the static pressure difference and plate spacing were obtained experimentally. These data are presented in graphical form and analyzed in order to select optimum plate spacing. It can be concluded from the present work that by invariably increasing the ΔP , the cooling rate cannot be enhanced continuously. There are some limitations imposed on the values of ΔP , after that it is advisable to incorporate some other technique other than mixed convection to increase the heat removal rate. Since for the uniform heat flux along the plate, the lower part surface temperature was less than the other part, so one should place the high heat flux components lower in the channel to work in the safe temperature range. As indicated earlier, for mixed convection through vertical rectangular ducts, there does not appear to be available any study corresponding to the case of uniform heat flux. As such, the accuracy of the present results was difficult to estimate, as no analytical model or the experimental data of other authors were available for the uniform heat flux situation.

5.10 Suggestions for Future Work

- A similar experimental work can be carried out for uniform temperature of the heated plate.
- The effect of plate inclination on the overall performance can be investigated.
- Present study does not consider the effects of surface roughness on overall performance. The model can be extended to find the effects of surface roughness on the heat transfer characteristics.
- The effects of discrete heat sources can also be investigated.

REFERENCES

- 1- Manca, O., Morrone, B. and Nardini, S., 2000, 'Experimental analysis of thermal instability in natural convection between horizontal parallel plates uniformly heated', *Journal of Heat Transfer*, Vol. 122, pp 50-57.
- 2- Sezai, I. and Monamd, A.A., 2000, 'Natural convection from a discrete heat source on the bottom of a horizontal enclosure', *Int. J. of Heat and Mass Transfer*, Vol. 43, pp 2257-2266.
- 3- Lee, K.T., 1999, 'Laminar natural convection heat and mass transfer in vertical rectangular ducts', *Int. J. of Heat and Mass Transfer*, Vol.42, pp 4523-4534.
- 4- Liu. Y. and Phan-Thein, N., 2000, 'An optimum spacing problem for three chips mounted on a vertical substrate in an enclosure, *Numerical Heat Transfer, Part A*, Vol. 37, pp 613-630.
- 5- Mendez, F. and Trevino, C., 2000, 'The conjugate conduction-natural convection heat transfer along a thin vertical plate with non-uniform internal heat generation', *Int. J. of Heat and mass Transfer*, Vol. 43, pp 2739-2748.
- 6- Chen, Y. -C. and Chung, J.N., 1998, 'Stability of mixed convection in a differently heated vertical channel', *Journal of Heat Transfer*, Vol. 120, pp 127-132.
- 7- Barletta, A., 2000, 'Combined forced and free flow of a power-law fluid in a vertical annular duct, *Int J. of Heat and Mass Transfer*, Vol. 43, pp 3673-3686.
- 8- Barletta, A., 1999, 'Analysis of combined forced and free flow in a vertical channel with viscous dissipation and isothermal-isoflux boundary conditions', *Journal of Heat Transfer*, Vol. 121, pp 349-357.

REFERENCES

- 1- Manca, O., Morrone, B. and Nardini, S., 2000, 'Experimental analysis of thermal instability in natural convection between horizontal parallel plates uniformly heated', *Journal of Heat Transfer*, Vol. 122, pp 50-57.
- 2- Sezai, I. and Monamd, A.A., 2000, 'Natural convection from a discrete heat source on the bottom of a horizontal enclosure', *Int. J. of Heat and Mass Transfer*, Vol. 43, pp 2257-2266.
- 3- Lee, K.T., 1999, 'Laminar natural convection heat and mass transfer in vertical rectangular ducts', *Int. J. of Heat and Mass Transfer*, Vol. 42, pp 4523-4534.
- 4- Liu. Y. and Phan-Thein, N., 2000, 'An optimum spacing problem for three chips mounted on a vertical substrate in an enclosure', *Numerical Heat Transfer, Part A*, Vol. 37, pp 613-630.
- 5- Mendez, F. and Trevino, C., 2000, 'The conjugate conduction-natural convection heat transfer along a thin vertical plate with non-uniform internal heat generation', *Int. J. of Heat and mass Transfer*, Vol. 43, pp 2739-2748.
- 6- Chen, Y. -C. and Chung, J.N., 1998, 'Stability of mixed convection in a differently heated vertical channel', *Journal of Heat Transfer*, Vol. 120, pp 127-132.
- 7- Barletta, A., 2000, 'Combined forced and free flow of a power-law fluid in a vertical annular duct', *Int. J. of Heat and Mass Transfer*, Vol. 43, pp 3673-3686.
- 8- Barletta, A., 1999, 'Analysis of combined forced and free flow in a vertical channel with viscous dissipation and isothermal-isoflux boundary conditions', *Journal of Heat Transfer*, Vol. 121, pp 349-357.

- 9- Moukalled, F., Doughan, A. and Acharya, S., 2000, 'Parametric study of mixed convection in channels with concave and convex surfaces', *Int. J. of Heat and Mass Transfer*, Vol. 43, pp 1947-1963.
- 10- Yadav, V. and Kant, K., 2000, 'Optimum static pressure in mixed convection cooling in a stack of heated plates', *Proceedings of the fourth ISHMT-ASME Heat and Mass Transfer Conference*, pp. 623-630.
- 11- Argento, W., joshi, Y.K. and Osterman, M.D., 1996, 'Forced convection air-cooling of a commercial electronic chassis: an experimental and computational case study, *IEEE Transaction on Components, Packaging and Manufacturing Technology, Part A*, Vol. 19, pp 248-257.
- 12- Coprland, K., 1998, 'Forced convection from rectangular arrays of electronic components', *Int. J. of Heat and Mass Transfer*, Vol. 41, pp 3219-3239.
- 13- Leung, C.W., Chen, S. and Chan, T.L., 2000, 'Numerical simulation of laminar forced convection in an air-cooled horizontal printed circuit board assembly', *Numerical Heat transfer, Part A*, Vol. 37, pp 373-393.
- 14- Young, T.J. and Vafai, K., 1998, 'Convective flow and heat transfer in a channel containing multiple heated obstacles', *Int. J. of Heat and Mass Transfer*, Vol.41, pp 3279-3298.
- 15- Tso, C.P., Xu, G.P. and Tou, K.W., 1999, 'An experimental study on forced convection heat transfer from flush-mounted discrete heat sources', *Journal of Heat Transfer*, Vol.121, pp 898-980.
- 16- Behnia, M., Dehghan, A.A., Mishima, H. and Nakayama, W., 1998, 'A numerical study of natural convection immersion cooling of multiple heat sources in parallel interacting open-top cavities', *Int. J. of Heat and Mass Transfer*, Vol. 41, pp 797-808.

- 17- Fedorov, A.G. and Viskanta, R., 2000,'Three-dimensional conjugate heat transfer in the microchannel heat sink for electronic packaging', *Int. J. of Heat and Mass Transfer*, Vol. 43, pp 399-415.
- 18- Lee, D. -Y. and Vafai, K., 1999,'Comparative analysis of jet impingement and micro channel cooling for high heat flux applications', *Int. J. of Heat and Mass transfer*, Vol. 42, pp 1555-1568.
- 19-Vafai, K. and Zhu, L., 1999,'Analysis of two-layered micro-channel heat sink concept in electronic cooling', *Int. J. of Heat and Mass Transfer*, Vol. 42, pp 2287-2297.
- 20- Kim, S.J., Kim, D. and Lee, D.Y., 2000,'on the local thermal equilibrium in micro channel heat sinks', *Int. J. of heat and Mass Transfer*, Vol. 43, pp 1735-1748.
- 21- Wolfersdorf, J.V., Achermann, E. and Weigand, B., 1997,'Shape optimization of cooling channels using *genetic algorithm*', *Journal of Heat Transfer*, Vol. 119, pp 380-388.
- 22- Greiner, M., Spencer, G.J. and Fisher, P.F., 1998,'Direct numerical simulation of three-dimensional flow and augmented heat transfer in a *grooved channel*', *Journal of Heat Transfer*, Vol.120, pp 717-734.
- 23- Katoh, K., Choi, K.S. and Azuma, T., 2000,'Heat-transfer enhancement and pressure loss by surface roughness in turbulent channel flows', *Int. J. of Heat and Mass Transfer*, Vol. 43, pp 4009-4017.
- 24- Cheng, C-H., Lin, C-Y. and Aung W., 2000,'Predictions of developing flow with buoyancy-assisted flow separation in a vertical rectangular duct: parabolic model versus elliptic model', *Numerical Heat Transfer, Part A*, Vol. 37, pp 567-586.

- 25- Choi, S.H., Shin, S. and Cho, Y.I., 1993, 'The effects of the Reynolds number and width ratio on the flow distribution in manifolds of liquid cooling modules for electronic packaging', *Int. Comm. Heat Mass Transfer*, Vol. 20, pp 607-617.
- 26- Jubran, B.A. and Al-Haroun, M.S., 1998, 'Heat transfer enhancement in electronic modules using various secondary air injection hole arrangements', *Journal of Heat Transfer*, Vol. 120, pp 342-348.
- 27- Fitzgerald, J.A. and Garimella, S.V., 1997, 'A study of the flow fields of a confined and submerged impinging jet', *Int. J. of Heat and Mass Transfer*, Vol. 41, pp 1025-1034.
- 28- Behmia, M., Parenix, S. and Dubrin, P.A., 1997, 'Prediction of heat transfer in an axisymmetric turbulent jet impinging on a flat plate', *Int. J. of Heat and Mass Transfer*, Vol. 41, pp 1845-1855.
- 29- Huang, L. and El-Genk, M.S., 1997, 'Heat transfer and flow visualization experiments of swirling, multi-channel, and conventional impinging jets', *Int. J. of Heat and Mass Transfer*, Vol. 41, pp 583-600.
- 30- Voke, P.R. and Gao, S., 1998, 'Numerical study of heat from an impinging jet', *Int. J. of Heat and Mass Transfer*, Vol. 41, pp 671-680.
- 31- Yao, L.S., 1983, 'Free and forced convection in the entry region of a heated vertical channel', *Int. J. Of Heat and mass Transfer*, Vol. 26, pp 65-72.
- 32- Dyer, J.R., and Fowler, J.H., 1966, 'The development of natural convection in a partially-heated vertical channel formed by two parallel surfaces', *Mech. and Chem. Energy Trans. MC2, Institution of Engineers(Australia)*, Vol.1, pp. 12-16.
- 33- William, H., Rae, and Pope, A., 'Low-speed wind tunnel testing', ed. Second, *John Wiley and Sons*, 1984.

APPENDIX 1

Variation of various parameters with plate spacing and pressure differential.

QAT= Total power input to plate A, W

QBT= Total power input to plate B, W

QAF= Heat flux from plate A, W/cm²

QBF= Heat flux from plate B, W/cm²

PF= Fan power input, W

Ti= Air inlet temperature, °C

Te= Air exit temperature, °C

ma= Mass flow rate of air, Kg/s.

Qc= Total heat transfer inside the channel, W

Qw= Total power input to both the plates, W.

ΔP=0.0 Pa

Spacing (x), m

	x1 =0.005	x2 =0.010	x3 =0.020	x4 =0.030	x5 =0.040	x6 =0.050	x7 =0.060	x8 =0.070	x9 =0.075
QAT=	88.9	97.1	140.9	147.2	142.5	168.3	170.7	212.8	196.4
QAF=	889.3	970.9	1409.3	1472.0	1424.6	1682.6	1706.6	2128.0	1963.8
QBT=	53.2	60.5	117.9	104.0	116.1	116.2	90.4	150.8	131.8
QBF=	532.5	604.8	1178.6	1040.0	1161.0	1161.6	904.3	1508.5	1317.8
PF=	0.0	0.0	0.0	0.0	0.0	0.0	0.0	0.0	0.0
Ti=	19.1	21.1	19.7	20.9	19.4	19.4	19.4	19.7	20.0
Te=	41.7	64.7	52.2	32.6	33.4	31.4	21.9	23.3	28.3
ma=	0.00213	0.00614	0.01671	0.02261	0.01606	0.01720	0.02212	0.02351	0.02458
Qc=	49.4	274.4	556.2	271.2	230.1	210.8	56.9	85.1	207.1
Qw=	142.2	157.6	258.8	251.2	258.6	284.4	261.1	363.6	328.2

ΔP=4.4 Pa

Spacing(x),m

	x1 =0.005	x2 =0.010	x3 =0.020	x4 =0.030	x5 =0.040	x6 =0.050	x7 =0.060	x8 =0.070	x9 =0.075
QAT=	266.0	183.4	283.7	249.5	290.6	333.6	289.7	286.4	274.0
QAF=	2659.5	1834.2	2836.8	2494.7	2906.2	3335.7	2897.3	2863.7	2740.2
QBT=	174.7	107.4	200.1	206.9	294.0	240.4	235.4	261.0	245.2
QBF=	1746.9	1073.9	2000.6	2069.1	2940.2	2403.8	2353.6	2610.2	2452.2
PF=	0.8	2.0	3.3	3.7	6.6	8.2	7.9	9.1	10.0
Ti=	20.9	22.7	21.7	20.8	19.6	21.1	21.3	20.6	21.6
Te=	56.5	62.5	43.8	36.8	39.2	36.6	30.2	24.6	28.6
ma=	0.00786	0.01573	0.03293	0.03342	0.05341	0.07946	0.09044	0.10895	0.12103
Qc=	287.1	640.7	746.2	544.9	1073.1	1261.9	824.7	443.3	875.2
Qw=	440.6	290.8	483.7	456.4	584.6	574.0	525.1	547.4	519.2

$\Delta P=8.8$ Pa

Spacing (x), m

	x1 =0.005	x2 =0.010	x3 =0.020	x4 =0.030	x5 =0.040	x6 =0.050	x7 =0.060	x8 =0.070	x9 =0.075
QAT=	235.0	246.0	417.3	474.3	447.8	449.1	270.7	291.6	400.1
QAF=	2349.8	2460.2	4172.8	4743.4	4478.1	4490.9	2706.9	2916.5	4000.6
QBT=	228.8	184.2	273.8	412.2	225.8	251.4	420.6	271.1	317.2
QBF=	2288.5	1841.6	2738.2	4121.9	2258.2	2513.6	4205.8	2711.0	3172.5
PF =	1.2	2.3	3.9	6.1	7.2	10.8	11.4	13.7	14.0
Ti =	19.1	22.5	21.9	21.1	21.2	22.2	19.4	20.7	21.6
Te =	46.3	55.1	39.3	37.1	34.2	32.2	27.2	25.5	27.9
ma =	0.01065	0.02236	0.02015	0.07004	0.08945	0.11264	0.12779	0.15712	0.16711
Qc =	297.5	745.3	359.7	1149.8	1186.6	1152.3	1022.8	783.1	1081.0
Qw =	463.8	430.2	691.1	886.5	673.6	700.4	691.3	562.8	717.3

APPENDIX 2

Variation of Nusselt number and Grashoff Number with plate spacing, x and plate height y*.

x, is plate spacing,

y*, is non-dimensional plate height,

Nu_y, is local Nusselt number,

Gr_y, is local Grashoff number.

$\Delta P=0.0$ Pa

x (cm)	y*	Nu _y	Gr _y
0.05	0.20	0.002155	1.08e+06
0.05	0.40	0.006779	2.95e+07
0.05	0.60	0.008869	1.42e+08
0.05	0.80	0.007501	3.96e+08
0.05	1.00	0.016755	8.82e+08
0.10	0.20	0.025639	1.43e+09
0.10	0.40	0.029673	2.40e+09
0.10	0.60	0.033039	3.61e+09
0.10	0.80	0.023634	5.20e+09
0.10	1.00	0.046363	6.45e+09
0.20	0.20	0.088680	1.00e+10
0.20	0.40	0.098081	1.32e+10
0.20	0.60	0.113788	1.71e+10
0.20	0.80	0.088618	2.19e+10
0.20	1.00	0.104334	2.74e+10
0.30	0.20	0.126527	3.09e+10
0.30	0.40	0.129630	3.70e+10
0.30	0.60	0.134761	4.38e+10
0.30	0.80	0.098167	5.58e+10
0.30	1.00	0.141137	6.64e+10
0.40	0.20	0.173418	7.41e+10
0.40	0.40	0.171925	8.77e+10
0.40	0.60	0.179880	9.67e+10
0.40	0.80	0.159409	1.14e+11
0.40	1.00	0.197804	1.31e+11
0.50	0.20	0.216951	1.43e+11
0.50	0.40	0.234079	1.54e+11
0.50	0.60	0.231481	1.74e+11
0.50	0.80	0.189103	2.09e+11
0.50	1.00	0.296265	1.75e+11
0.60	0.20	0.202583	2.59e+11
0.60	0.40	0.206013	2.80e+11
0.60	0.60	0.177899	3.20e+11
0.60	0.80	0.154346	3.33e+11
0.60	1.00	0.280912	2.83e+11
0.70	0.20	0.370318	3.92e+11
0.70	0.40	0.378791	4.16e+11
0.70	0.60	0.384435	4.54e+11
0.70	0.80	0.378518	4.89e+11

0.70	1.00	0.450879	4.78e+11
0.75	0.20	0.349629	6.10e+11
0.75	0.40	0.365120	6.42e+11
0.75	0.60	0.363757	6.83e+11
0.75	0.80	0.335885	7.29e+11
0.75	1.00	0.478563	6.58e+11

$\Delta P=4.4$ Pa

x (cm)	y*	Nu _y	Gr _y
0.05	0.20	0.678694	6.72e+11
0.05	0.40	0.651056	7.25e+11
0.05	0.60	0.662076	8.41e+11
0.05	0.80	0.573613	9.59e+11
0.05	1.00	0.561729	1.10e+12
0.10	0.20	0.449119	9.54e+11
0.10	0.40	0.371621	1.25e+12
0.10	0.60	0.414593	1.12e+12
0.10	0.80	0.339650	1.25e+12
0.10	1.00	0.478550	1.20e+12
0.20	0.20	0.803576	1.42e+12
0.20	0.40	0.747959	1.54e+12
0.20	0.60	0.804798	1.65e+12
0.20	0.80	0.732168	1.80e+12
0.20	1.00	0.826931	1.92e+12
0.30	0.20	0.971503	1.68e+12
0.30	0.40	0.906385	1.90e+12
0.30	0.60	0.942479	1.99e+12
0.30	0.80	0.912766	2.19e+12
0.30	1.00	1.001904	2.12e+12
0.40	0.20	1.563014	2.29e+12
0.40	0.40	1.460272	2.55e+12
0.40	0.60	1.302936	2.71e+12
0.40	0.80	1.191881	3.00e+12
0.40	1.00	1.279232	3.08e+12
0.50	0.20	1.238241	2.70e+12
0.50	0.40	1.248082	2.87e+12
0.50	0.60	1.208007	3.24e+12
0.50	0.80	1.230326	3.44e+12
0.50	1.00	1.472196	3.08e+12
0.60	0.20	1.283172	3.41e+12
0.60	0.40	1.295138	3.59e+12
0.60	0.60	1.230871	3.91e+12
0.60	0.80	1.300688	4.14e+12
0.60	1.00	1.519669	3.71e+12
0.70	0.20	1.488131	4.38e+12
0.70	0.40	1.473367	4.54e+12
0.70	0.60	1.410571	5.16e+12
0.70	0.80	1.522968	5.39e+12
0.70	1.00	1.523946	4.78e+12
0.75	0.20	1.516937	5.10e+12
0.75	0.40	1.490085	5.20e+12
0.75	0.60	1.437739	5.97e+12
0.75	0.80	1.520305	6.08e+12
0.75	1.00	1.481922	6.46e+12

$\Delta P=8.8 \text{ Pa}$

x (cm)	y*	Nu _y	Gr _y
0.05	0.20	1.649867	5.31e+12
0.05	0.40	1.652046	5.73e+12
0.05	0.60	1.521847	6.60e+12
0.05	0.80	1.533191	7.30e+12
0.05	1.00	1.495405	8.05e+12
0.10	0.20	1.440860	6.22e+12
0.10	0.40	1.292694	7.06e+12
0.10	0.60	1.306008	7.23e+12
0.10	0.80	1.278170	7.92e+12
0.10	1.00	1.392033	7.68e+12
0.20	0.20	2.217859	7.35e+12
0.20	0.40	2.005467	8.03e+12
0.20	0.60	1.944033	9.02e+12
0.20	0.80	2.018815	9.66e+12
0.20	1.00	1.955692	1.02e+13
0.30	0.20	3.004232	9.55e+12
0.30	0.40	2.857215	1.04e+13
0.30	0.60	2.942721	1.08e+13
0.30	0.80	3.531475	1.08e+13
0.30	1.00	2.947737	1.18e+13
0.40	0.20	1.975303	1.00e+13
0.40	0.40	1.907778	1.05e+13
0.40	0.60	1.846056	1.17e+13
0.40	0.80	1.757123	1.25e+13
0.40	1.00	1.822335	1.27e+13
0.50	0.20	2.369820	1.09e+13
0.50	0.40	2.175297	1.17e+13
0.50	0.60	2.098493	1.30e+13
0.50	0.80	2.170027	1.41e+13
0.50	1.00	2.444337	1.27e+13
0.60	0.20	2.217880	1.45e+13
0.60	0.40	2.288508	1.54e+13
0.60	0.60	7.936914	1.68e+13
0.60	0.80	2.562187	1.88e+13
0.60	1.00	2.130251	1.76e+13
0.70	0.20	2.495894	1.55e+13
0.70	0.40	2.136642	1.88e+13
0.70	0.60	2.351346	1.80e+13
0.70	0.80	2.500433	1.87e+13
0.70	1.00	2.686413	1.71e+13
0.75	0.20	3.038859	1.70e+13
0.75	0.40	2.969691	1.78e+13
0.75	0.60	2.734825	2.03e+13
0.75	0.80	3.102233	2.09e+13
0.75	1.00	3.180824	1.94e+13

133714
Date Slip

[illegible]